

# S.M. Higgs Decay and Production Channels

Trabajo Fin de Master 2010 - 2011

Victor Ilisie

tutor: **Antonio Pich Zardoya**

Universidad de Valencia, Septiembre 2011

## **Abstract:**

As the first part of this paper we get to analyze Standard Model (SM) Higgs boson main decay channels, at tree level for massive final state particles and at one loop for gluons. We reproduce also the plot for Higgs branching ratios for different decay channels as a function of its mass. Next we get to analyze the LHC and Tevatron main Higgs production channels, gluon-gluon fusion, weak boson fusion and Higgs-strahlung. We numerically integrate the obtained cross sections convoluted with the parton distribution functions (PDFs) in order to obtain a realistic leading order (LO) estimation of the result. At this point, we analyze an extended version of the SM with a fourth generation of leptons and quarks (SM4). We compare the SM4 theoretical predictions with the latest experimental results and get to an interesting conclusion. Afterwards, we will also analyze one loop Higgs self-energy diagrams and see how the Higgs running mass looks like, and draw another interesting conclusion about the SM at higher energy scales. Last, we take a look at the latest experimental results on Higgs mass exclusion regions.

## Table of Contents:

<b>0. The Standard Model</b>	3
<b>1. Higgs Decay Channels</b>	4
1.1 Higgs decay to fermion-antifermion	4
1.2 Higgs decay to weak bosons	5
1.3 Two gluons Higgs decay	6
1.4 Three body Higgs decay	10
<b>2. Higgs Production Channels</b>	17
2.1 Gluon-gluon fusion	17
2.2 Weak boson fusion	17
2.3 Higgs-strahlung	21
2.4 Parton distribution functions and Integrated Cross Sections	23
2.5 Fourth generation SM Extension (SM4)	30
<b>3. Higgs Mass Renormalization</b>	32
3.1 Optical Theorem	33
3.2 Self energy diagrams	35
3.7 Higgs running mass	44
<b>46. Final Conclusions</b>	46
<b>5. References</b>	49

## 0. Standard Model

Since the discovery of the  $\beta$  decay of neutrons, many efforts have been made to understand the nature of the weak interaction. The development of a formal consistent theory of this interaction had to pass through many stages and tests. The first model capable of describing successfully the experimental data at low energies was the effective interaction proposed by Fermi in 1934:

$$\mathcal{L}_{eff}(x) = \frac{G_F}{\sqrt{2}} J_\mu^\dagger(x) J^\mu(x) \quad (0.1)$$

this is a current-current interaction with  $J^\mu$  given by:

$$J^\mu(x) = \sum_l \bar{\nu}_l(x) \gamma^\mu (1 - \gamma_5) l(x) + \bar{p}(x) \gamma^\mu (1 - \gamma_5) n(x) \quad (0.2)$$

The first part is the leptonic part and the second one was naively thought to be the part describing the interaction between nucleons. Nowadays we know that we have to substitute the nucleon fields for quark fields. Let's take a look at the simplest cross section we can imagine calculated with Fermi's interaction lagrangian:

$$\sigma(\nu_\mu e^- \rightarrow \nu_e \mu^-) = \frac{G_F^2 s}{\pi} \sim s \quad (0.3)$$

Obviously, as we mentioned before, this theory can only describe low energy phenomenology; at high enough energies it violates unitarity. The other problem that makes this theory ill is that it's non renormalizable. All higher order corrections are found to be infinite. A theory is called renormalizable if all ultraviolet divergences can be reabsorbed in a redefinition of the coupling constants and fields. With Fermi's theory this is impossible. The next step was the Intermediate Vector Boson (IVB) theory. Here we assume that the weak interaction is mediated by a vector boson, analogous to QED, but in this case it would have to be a massive boson because of the short range of the interaction.

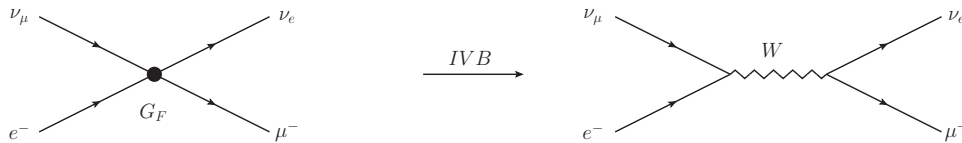


Figure 1: Fermi's effective coupling and the IVB theory.

This theory was also doomed to fail. One can easily find that this theory again violates unitarity and is non-renormalizable. Finally, in 1967, Weinberg, Salam and Glashow proposed an electro-weak unified theory which successfully passed almost all the tests. This theory is what we now call the Standard Model of Electroweak Interactions. It is a gauge theory based on the symmetry group  $SU(2)_L \otimes U(1)_Y$  with massless particles. Together with the strong interaction we have the  $SU(3)_C \otimes SU(2)_L \otimes U(1)_Y$  group which describes the whole SM. The mechanism that provides mass to all the particles is called Spontaneous Symmetry Breaking (SSB):

$$SU(3)_C \otimes SU(2)_L \otimes U(1)_Y \rightarrow SU(3)_C \otimes U(1)_{QED}$$

The SSB is generated by the non-zero expectation value of a  $SU(2)$  doublet which is called Higgs doublet. This doublet also gives rise to a scalar particle, the Higgs boson, which couples to all massive fields in the theory. So far, the SM has been very successful and it passed many precision tests. The only ingredient left to be discovered, if it exists, is the scalar Higgs boson. This paper will be dedicated to the analysis of this particle. In order to get an idea of the underlying physics of the Higgs boson we have to study at least three things: decay channels, production mechanisms at particle colliders such as the LHC and Tevatron, and of course, renormalization. We shall start by analyzing its decay channels in the next section.

# 1. Higgs Decay Channels

The first thing that we have to do in order to get a correct and complete vision of the Higgs phenomenology is to analyze at tree level it's coupling to all the massive particles in the S.M. We shall start by analyzing the fermion anti-fermion channels and the weak boson channels. Afterwards we also need to analyze massless final state bosons like gluons or photons. We can argue that  $\gamma\gamma$  and  $\gamma Z$  final states are very small compared to all the others so we could leave them out of our discussion, but we are going to include them anyway (from ref.[16]) for completeness sake and also because  $H \rightarrow \gamma\gamma$  is a very interesting channel for a low mass Higgs. These processes and  $H \rightarrow gg$  take place through loop diagrams. We will see that the loop diagrams need to be taken in consideration for a correct understanding of the Higgs phenomenology.

## 1.1 Higgs decay to fermion anti-fermion.

$H(p_1) \rightarrow f(p_2)\bar{f}(p_3)$ :

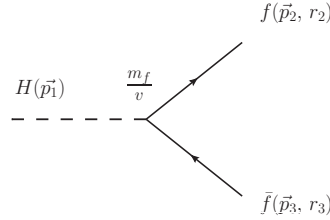


Figure 2: Higgs decay to fermions.

The transition amplitude of this diagram is given by :

$$\mathcal{M}_{H \rightarrow f\bar{f}} = \frac{m_f}{v} \bar{u}_{r_2} v_{r_3} \Rightarrow \mathcal{M}_{H \rightarrow f\bar{f}}^\dagger = \frac{m_f}{v} \bar{v}_{r_3} u_{r_2} \quad (1.1)$$

Therefore the squared transition amplitude is:

$$\sum_{r_2, r_3} |\mathcal{M}_{H \rightarrow f\bar{f}}^2| = \frac{m_f^2}{v^2} \text{Tr}\{(p_2 + m_f)(p_3 - m_f)\} = \frac{4m_f^2}{v^2} (p_2 p_3 - m_f^2) \quad (1.2)$$

In the center of mass frame the relativistic four-momenta are given by:

$$p_1^\mu = (M_H, \vec{0}), \quad p_2^\mu = (E_f, \vec{p}), \quad p_3^\mu = (E_f, -\vec{p}) \quad (1.3)$$

where, momentum conservation implies:

$$M_H = 2E_f \text{ with } E_f^2 = p^2 + m_f^2, \quad p = |\vec{p}| \quad (1.4)$$

We can easily find that:

$$p_2 p_3 - m_f^2 = \frac{1}{2} M_H^2 \left(1 - \frac{4m_f^2}{M_H^2}\right); \quad p = \frac{1}{2} M_H \left(1 - \frac{4m_f^2}{M_H^2}\right)^{1/2} \quad (1.5)$$

and we also find the squared amplitude of the process to be:

$$\sum_{r_i} |M_{(H \rightarrow f\bar{f})}|^2 = N_C \frac{2m_f^2}{v^2} M_H^2 \left(1 - \frac{4m_f^2}{M_H^2}\right) \quad (1.6)$$

The decay width is defined by the formula (X, X' can be anything):

$$\Gamma(H \rightarrow XX') \equiv \frac{1}{2M_H} \int dQ_2 \sum |M_{(H \rightarrow XX')}|^2 \quad (1.7)$$

In this case the transition amplitude does not depend on any angle, so it can be directly integrated:

$$\int dQ_2 = \int \frac{1}{(2\pi)^2} \frac{p}{4\sqrt{s}} d\Omega_{CM} = \frac{1}{8\pi} \left(1 - \frac{4m_f^2}{M_H^2}\right)^{1/2} \quad (1.8)$$

Therefore, the partial decay width of the Higgs boson to fermion anti-fermion is:

$$\Gamma(H \rightarrow f\bar{f}) = N_C \frac{1}{8\pi} \frac{m_f^2}{v^2} M_H \left(1 - \frac{4m_f^2}{M_H^2}\right)^{3/2} \quad (1.9)$$

$N_C$  is the number of colours; it's value is 1 for leptons and 3 for quarks.

### 1.2 Higgs decay to weak bosons.

$H(p_1) \rightarrow Z(p_2)Z(p_3)/W(p_2)W(p_3)$ :

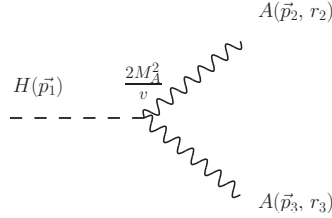


Figure 3: Higgs decay to weak bosons  $A = W, Z$ .

We shall calculate the transition amplitude with a general weak boson  $\mathbf{A}$  which can be either one. Afterwards we shall particularize the result for each one of them, considering that in phase space the  $ZZ$  decay width has an extra  $1/2$  identical particles factor. The transition amplitude of this diagram is therefore given by :

$$\mathcal{M}_{H \rightarrow AA} = \frac{2M_A^2}{v} \epsilon_{r_2}^\mu \epsilon_{\mu, r_3} \Rightarrow \mathcal{M}_{H \rightarrow AA}^\dagger = \frac{2M_A^2}{v} \epsilon_{r_2}^{\nu*} \epsilon_{\nu, r_3}^* \quad (1.10)$$

We find the squared transition amplitude to be:

$$\sum_{r_i} |\mathcal{M}_{H \rightarrow AA}|^2 = \frac{4M_A^4}{v^2} \left( -g^{\mu\nu} + \frac{p_2^\mu p_2^\nu}{M_A^2} \right) \left( -g_{\mu\nu} + \frac{p_{3\mu} p_{3\nu}}{M_A^2} \right) \quad (1.11)$$

Considering the the final vector bosons are on-shell, the squared amplitude becomes:

$$\sum_{r_i} |\mathcal{M}_{H \rightarrow AA}|^2 = \frac{4M_A^4}{v^2} \left( 2 + \frac{(p_2 p_3)^2}{M_A^4} \right) = \frac{4M_A^4}{v^2} \left( 3 + \frac{1}{4} \frac{M_H^4}{M_A^4} - \frac{M_H^2}{M_A^2} \right) \quad (1.12)$$

We have the same two-particle phase space as in the previous example (except the  $1/2$  factor that goes to  $ZZ$ , and different masses) so the partial decay rate of the Higgs boson to Weak bosons  $W$  or  $Z$  is:

$$\Gamma(H \rightarrow WW) = \frac{1}{4\pi} \frac{M_W^4}{M_H v^2} \left( 1 - \frac{4M_W^2}{M_H^2} \right)^{1/2} \left( 3 + \frac{1}{4} \frac{M_H^4}{M_W^4} - \frac{M_H^2}{M_W^2} \right) \quad (1.13)$$

$$\Gamma(H \rightarrow ZZ) = \frac{1}{8\pi} \frac{M_Z^4}{M_H v^2} \left( 1 - \frac{4M_Z^2}{M_H^2} \right)^{1/2} \left( 3 + \frac{1}{4} \frac{M_H^4}{M_Z^4} - \frac{M_H^2}{M_Z^2} \right) \quad (1.14)$$

### 1.3 Higgs decay to gluons.

The next process is a one-loop process. We could naively think that its decay rate must be very low compared to the tree-level ones, but that is not exactly true. Due to the very heavy top quark mass, this diagram generates a high enough decay rate that necessarily must be taken in consideration. We shall see at the end of our computation that for a massless quark this diagram does not contribute.

$H(p_1) \rightarrow g(p_2)g(p_3)$

**first diagram:**

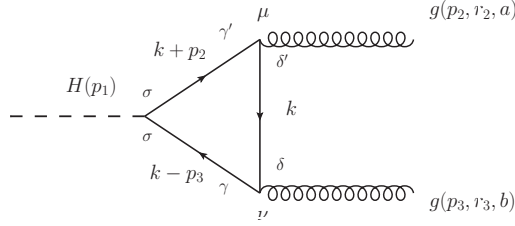


Figure 4: Higgs decay to gluons, first diagram.

The transition amplitude of the first diagram is given by:

$$\begin{aligned} \mathcal{M}_{(1)} = & (-i)g_s^2 \frac{m}{v} \epsilon_{\mu, r_2}^a \epsilon_{\nu, r_3}^b \left(\frac{\lambda^a}{2}\right)_{\delta' \gamma'} \left(\frac{\lambda^b}{2}\right)_{\gamma \delta} \delta_{\delta \delta'} \delta_{\gamma' \sigma} \delta_{\sigma \gamma} \times \\ & \int \frac{d^4 k}{(2\pi)^4} \frac{\text{Tr}\{\gamma^\mu (\not{k} + \not{p}_2 + m)(\not{k} - \not{p}_3 + m)\gamma^\nu (\not{k} + m)\}}{(k^2 - m^2)[(k + p_2)^2 - m^2][(k - p_3)^2 - m^2]} \end{aligned} \quad (1.15)$$

Here  $m = m_t$ , the top quark mass. Let's first analyze the colour trace:

$$\left(\frac{\lambda^a}{2}\right)_{\delta' \gamma'} \left(\frac{\lambda^b}{2}\right)_{\gamma \delta} \delta_{\delta \delta'} \delta_{\gamma' \sigma} \delta_{\sigma \gamma} = \frac{1}{4} \text{Tr}\{\lambda^a \lambda^b\} = \frac{1}{2} \delta_{ab} \quad (1.16)$$

The spinor trace is a little more complicated:

$$\begin{aligned} & \text{Tr}\{\gamma^\mu (\not{k} + \not{p}_2 + m)(\not{k} - \not{p}_3 + m)\gamma^\nu (\not{k} + m)\} \\ & = 4m(p_3^\mu p_2^\nu + 4k^\mu k^\nu - 2k^\mu p_3^\nu + 2p_2^\mu k^\nu - p_2^\mu p_3^\nu + g^{\mu\nu}(m^2 - p_2 p_3) - g^{\mu\nu} k^2) \\ & \equiv 4mN^{\mu\nu} \end{aligned} \quad (1.17)$$

Before we try to perform the integral, we shall use the Feynman parameterization to simplify the denominator:

$$\frac{1}{ABC} = \int_0^1 dx \int_0^1 dy \int_0^1 dz \delta(x + y + z - 1) \frac{2}{[Ax + By + Cz]^3} \quad (1.18)$$

We have,  $A = k^2 - m^2$ ,  $B = (k + p_2)^2 - m^2$  and  $C = (k - p_3)^2 - m^2$ , so the denominator  $\mathbf{D} \equiv \mathbf{Ax} + \mathbf{By} + \mathbf{Cz}$  can be written as it follows (as a first order approximation we shall consider **on-shell gluons**):

$$\begin{aligned} D & = (k^2 - m^2)x + (k^2 + p_2^2 - m^2 + 2kp_2)y + (k^2 + p_1^2 - m^2 - 2kp_3)z \\ & = (k^2 - m^2)(x + y + z) + 2(kp_2)y - 2(kp_3)z \\ & = k^2 - m^2 + 2(kp_2)y - 2(kp_3)z \\ & = (k + p_2y - p_3z)^2 + 2(p_2p_3)yz - m^2 \end{aligned} \quad (1.19)$$

We define  $\mathbf{a}^2 \equiv \mathbf{m}^2 - \mathbf{2(p_2p_3)yz}$ , therefore, we can write D in the simplified form :

$$D = (k + p_2y - p_3z)^2 - a^2 \quad (1.20)$$

In terms of the Feynman parameters, our integral becomes:

$$I^{\mu\nu} \equiv \int \frac{d^4k}{(2\pi)^4} \int_0^1 dy \int_0^{1-y} dz \frac{8mN^{\mu\nu}}{[(k + p_2y - p_3z)^2 - a^2]^3} \quad (1.21)$$

Making a variable shift from  $k$  to  $k + p_2y + p_3z$ ,  $I^{\mu\nu}$  takes the form:

$$I^{\mu\nu} = \int \frac{d^4k}{(2\pi)^4} \int_0^1 dy \int_0^{1-y} dz \frac{8mN'^{\mu\nu}}{(k^2 - a^2)^3} \quad (1.22)$$

Where the new numerator is:

$$N'^{\mu\nu} = 4(k - p_2y + p_3z)^\mu (k - p_2y + p_3z)^\nu - 2(k - p_2y + p_3z)^\mu p_3^\nu + 2p_2^\mu (k - p_2y + p_3z)^\nu + p_3^\mu p_2^\nu - p_2^\mu p_3^\nu + g^{\mu\nu}(m^2 - p_2p_3) - g^{\mu\nu}(k - p_2y + p_3z)^2 \quad (1.23)$$

Knowing that all terms that are linear in  $k^\mu$  vanish when integrated ( $k^\mu$  is an odd function) we can discard them from  $N'^{\mu\nu}$ , so what we have left is:

$$N'^{\mu\nu} = 4k^\mu k^\nu - g^{\mu\nu}k^2 + p_3^\mu p_2^\nu (1 - 4yz) + p_2^\mu p_3^\nu (-1 - 4yz + 2y + 2z) + p_3^\mu p_3^\nu (4z^2 - 2z) + p_2^\mu p_2^\nu (4y^2 - 2y) + g^{\mu\nu}(m^2 - p_2p_3 + 2p_2p_3yz) \quad (1.24)$$

There are a couple terms that are apparently ultraviolet divergent, such as  $4k^\mu k^\nu - g^{\mu\nu}k^2$  so we need to employ dimensional regularization to perform the four-momentum integral. We will also use the same technique to calculate the finite integrals. The scheme used here is the  $\overline{MS}$ , so we take the identity matrix trace in  $\mathbf{D}$  space-time dimensions to be 4 ( $Tr\{I_D\} = 4$ ). Now let us define the following integral:

$$J(D, \alpha, \beta, a^2) \equiv \int \frac{d^Dk}{(2\pi)^D} \frac{(k^2)^\alpha}{(k^2 - a^2)^\beta} \quad (1.25)$$

where  $\mathbf{D}$  is the number of space-time dimensions. We can easily show that:

$$J(D, \alpha, \beta, a^2) = \frac{i}{(4\pi)^{D/2}} (a^2)^{D/2} (-a^2)^{\alpha-\beta} \frac{\Gamma(\beta - \alpha - D/2)\Gamma(\alpha + D/2)}{\Gamma(\beta)\Gamma(D/2)} \quad (1.26)$$

All terms that do not depend on the four momentum  $k^\mu$  in the numerator give rise to finite integrals, thus in this case we can directly take  $\mathbf{D}$  as 4; so  $J(4, 0, 3, a^2)$  takes the simple form:

$$J(4, 0, 3, a^2) = \frac{-i}{32\pi^2} \frac{1}{a^2} \quad (1.27)$$

Due to Lorentz symmetry, we find the following property:

$$\int \frac{d^Dk}{(2\pi)^D} \frac{(k^2)^\alpha k^\mu k^\nu}{(k^2 - a^2)^\beta} = \frac{g^{\mu\nu}}{D} J(D, \alpha + 1, \beta, a^2) \quad (1.28)$$

Using this property we are now able to integrate the terms  $4k^\mu k^\nu - g^{\mu\nu}k^2$  from  $N'^{\mu\nu}$ :

$$\begin{aligned} \int \frac{d^Dk}{(2\pi)^D} \frac{4k^\mu k^\nu - g^{\mu\nu}k^2}{(k^2 - a^2)^3} &= \left(\frac{4}{D} - 1\right) g^{\mu\nu} J(D, 1, 3, a^2) \\ &= \left(\frac{4}{D} - 1\right) g^{\mu\nu} \frac{i}{(4\pi)^{D/2}} (a^2)^{D/2} (-a^2)^{-2} \frac{\Gamma(2 - D/2)\Gamma(1 + D/2)}{\Gamma(3)\Gamma(D/2)} \\ &= \left(\frac{4}{D} - 1\right) g^{\mu\nu} \frac{i}{(4\pi)^{D/2}} (a^2)^{D/2} \left(\frac{D}{4}\right) \Gamma(2 - D/2) \end{aligned} \quad (1.29)$$

Taking  $\mathbf{D} = 4 + 2\epsilon$  with  $\epsilon \ll 1$  we find:

$$\begin{aligned} \left(\frac{4}{D} - 1\right) \frac{D}{4} &= -\frac{\epsilon}{2} \\ \Gamma(2 - D/2) &= \Gamma(-\epsilon) = -\frac{1}{\epsilon} - \gamma_E + O(\epsilon^2) \end{aligned} \quad (1.30)$$

where  $\gamma_E$  is the Euler-Mascheroni constant. Substituting this result in our integral the pole of the Gamma function disappears therefore the ultraviolet divergence disappears. We can now take the limit  $\epsilon \rightarrow 0$  to obtain:

$$\int \frac{d^D k}{(2\pi)^D} \frac{4k^\mu k^\nu - g^{\mu\nu} k^2}{(k^2 - a^2)^3} = \frac{i}{32\pi^2} g^{\mu\nu} = \frac{i}{32\pi^2} \frac{a^2}{a^2} g^{\mu\nu} \quad (1.31)$$

We obtain the following expression for  $I^{\mu\nu}$ :

$$I^{\mu\nu} = \frac{8im}{32\pi^2} \int_0^1 \int_0^{1-y} \frac{dy dz}{-a^2} [p_2^\mu p_2^\nu (4y^2 - 2y) + p_3^\mu p_3^\nu (4z^2 - 2z) + p_3^\mu p_2^\nu (1 - 4yz) + p_2^\mu p_3^\nu (-4yz + 2y + 2z - 1) + g^{\mu\nu} (4p_2 p_3 y z - p_2 p_3)] \quad (1.32)$$

Now let us remember that we have considered on-shell gluons, therefore we can apply the transversality condition to eliminate terms from  $I^{\mu\nu}$ , thus keeping in mind that  $\epsilon_{\mu, r_i}^\mu = 0$  with  $i=2,3$ , then the only remaining tensorial structure is the following:

$$I^{\mu\nu} = \frac{8im}{32\pi^2} \int_0^1 \int_0^{1-y} \frac{dy dz}{-a^2} [p_3^\mu p_2^\nu (1 - 4yz) + g^{\mu\nu} (4p_2 p_3 y z - p_2 p_3)] \quad (1.33)$$

Rearranging terms we can write the following:

$$I^{\mu\nu} = \frac{8im}{32\pi^2} \int_0^1 \int_0^{1-y} \frac{dy dz}{-a^2} [p_3^\mu p_2^\nu - g^{\mu\nu} p_2 p_3] (1 - 4yz) \quad (1.34)$$

To simplify our notation let us define the following:

$$\int_0^1 \int_0^{1-y} dy dz \frac{1 - 4yz}{-a^2} \equiv C \quad (1.35)$$

Now we can write  $I^{\mu\nu}$  in a simple compact form:

$$I^{\mu\nu} = \frac{8im}{32\pi^2} C [p_3^\mu p_2^\nu - g^{\mu\nu} p_2 p_3] \quad (1.36)$$

Finally, we write the transition amplitude  $\mathcal{M}_{(1)}$ :

$$\mathcal{M}_{(1)} = (-i) g_s^2 \frac{m_t}{2v} \epsilon_{\mu, r_2}^a \epsilon_{\nu, r_3}^b \delta_{ab} I^{\mu\nu} \quad (1.37)$$

**second diagram:**

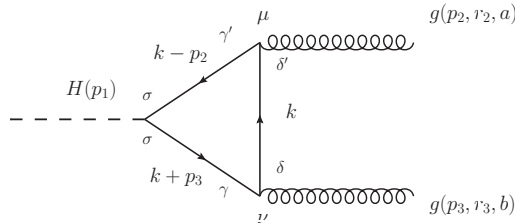


Figure 5: Higgs decay to gluons, second diagram.

The transition amplitude of this second diagram is given by:

$$\mathcal{M}_{(2)} = (-i)g_s^2 \frac{m}{2v} \epsilon_{\mu,r_2}^a \epsilon_{\nu,r_3}^b \delta_{ab} \int \frac{d^4k}{(2\pi)^4} \frac{\text{Tr}\{\gamma^\mu(\not{k}+m)\gamma^\nu(\not{k}+\not{p}_3+m)(\not{k}-\not{p}_2+m)\}}{(k^2-m^2)[(k-p_2)^2-m^2][(k+p_3)^2-m^2]} \quad (1.38)$$

Computing the spinor trace, and D in terms of the Feynman parameters we find:

$$\begin{aligned} & \text{Tr}\{\gamma^\mu(\not{k}+m)\gamma^\nu(\not{k}+\not{p}_3+m)(\not{k}-\not{p}_2+m)\} \\ &= 4m(p_3^\mu p_2^\nu + 4k^\mu k^\nu + 2k^\mu p_3^\nu - 2p_2^\mu k^\nu - p_2^\mu p_3^\nu + g^{\mu\nu}(m^2 - p_2 p_3 - k^2)) \\ &\equiv 4mM^{\mu\nu} \end{aligned} \quad (1.39)$$

and also, the following integral:

$$J^{\mu\nu} \equiv \int \frac{d^4k}{(2\pi)^4} \int_0^1 dy \int_0^{1-y} dz \frac{8mM^{\mu\nu}}{[(k-p_2y+p_3z)^2 - a^2]^3} \quad (1.40)$$

Performing the parameter shift  $k \rightarrow k - p_2y + p_3z$ ,  $J^{\mu\nu}$  takes the form:

$$J^{\mu\nu} \equiv \int \frac{d^4k}{(2\pi)^4} \int_0^1 dy \int_0^{1-y} dz \frac{8mM'^{\mu\nu}}{[k^2 - a^2]^3} \quad (1.41)$$

with the non zero contributing terms of  $M'^{\mu\nu}$ :

$$\begin{aligned} M'^{\mu\nu} &= p_2^\mu p_2^\nu (4y^2 - 2y) + p_3^\mu p_3^\nu (4z^2 - 2z) + p_3^\mu p_2^\nu (1 - 4yz) \\ &+ p_2^\mu p_3^\nu (-4yz + 2y + 2z - 1) + g^{\mu\nu}(2p_2 p_3 yz + m^2 - p_2 p_3) \\ &\equiv N'^{\mu\nu} \end{aligned} \quad (1.42)$$

So we find that  $I^{\mu\nu} = J^{\mu\nu}$ , therefore the amplitude of the second diagram is exactly the same as the first one  $\mathcal{M}_{(1)} = \mathcal{M}_{(2)}$ ; the total squared amplitude is then given by:

$$|\mathcal{M}|^2 = 4|\mathcal{M}_{(1)}|^2 \quad (1.43)$$

The sum over spins and gluon colours gives:

$$\sum_{a,b} \delta_{ab} \delta_{ab} = \sum_a \delta_{aa} = 8; \quad \sum_{r_2, r_3} \epsilon_{\rho, r_2}^{a*} \epsilon_{\mu, r_2}^a \epsilon_{\sigma, r_3}^{b*} \epsilon_{\nu, r_3}^b = g_{\mu\rho} g_{\sigma\nu} \quad (1.44)$$

We obtain the simple formula:

$$\sum_{r_2, r_3} |\mathcal{M}_{H \rightarrow gg}|^2 = g_s^4 \frac{8m^2}{v^2} I^{\mu\nu} I_{\mu\nu}^*; \quad I^{\mu\nu} I_{\mu\nu}^* = \frac{m^2 (p_2 p_3)^2 |C|^2}{8\pi^4} \quad (1.45)$$

The squared amplitude than reads:

$$\sum_{r_2, r_3} |\mathcal{M}_{H \rightarrow gg}|^2 = g_s^4 \frac{m^4 (p_2 p_3)^2}{v^2 \pi^4} |C|^2 \quad (1.46)$$

Let's compute now the integral **C** explicitly:

$$\begin{aligned} C &= \int_0^1 \int_0^{1-y} dy dz \frac{1-4yz}{-a^2} = \int_0^1 \int_0^{1-y} dy dz \frac{1-4yz}{2p_2 p_3 yz - m^2} = \frac{1}{2p_2 p_3} \int_0^1 \int_0^{1-y} dy dz \frac{1-4yz}{yz - \frac{m^2}{2p_2 p_3}} \\ &= \frac{1}{2p_2 p_3} \left[ -2 + (4n-1) \left( Li_2\left(\frac{-2}{\sqrt{1-4n}-1}\right) + Li_2\left(\frac{2}{\sqrt{1-4n}+1}\right) \right) \right] \\ &\equiv \frac{1}{2p_2 p_3} D(n) = \frac{n}{m^2} D(n) \end{aligned} \quad (1.47)$$

were we have defined  $\mathbf{n} \equiv \mathbf{m}^2/2\mathbf{p}_2\mathbf{p}_3$ . Taking the limit  $\lim_{m \rightarrow 0} \mathbf{n} \mathbf{D}(\mathbf{n})$  we observe that the result is zero, therefore, if we consider massless quarks as usual, except for the top quark, we only have one contribution, as we mentioned at the beginning. Moving on, in the center of mass the four-momenta are given by:

$$p_1^\mu = (M_H, \vec{0}), p_2^\mu = (p, \vec{p}), p_3^\mu = (p, -\vec{p}) \quad (1.48)$$

We can easily find that:

$$M_H = 2p \rightarrow p^2 = \frac{1}{4}M_H^2 \rightarrow p_2p_3 = 2p^2 = \frac{1}{2}M_H^2 \quad (1.49)$$

Therefore we can write the squared transition amplitude as:

$$\sum_{r_2, r_3} |\mathcal{M}_{H \rightarrow gg}|^2 = \frac{4M_H^4}{v^2} \left(\frac{\alpha_s}{\pi}\right)^2 n^2 |D(n)|^2 \quad (1.50)$$

The phase space integral is easy to compute:

$$\int dQ_2 = \frac{1}{2} \int \frac{1}{(2\pi)^2} \frac{p}{4\sqrt{s}} d\Omega_{CM} = \frac{1}{16\pi} \quad (1.51)$$

Note that we have included the symmetry factor 1/2 in the phase space integral because this time we are dealing with identical final state particles. Thus, the decay width of the process is given by ( $\mathbf{n} = \mathbf{m}^2/M_H^2$ ):

$$\Gamma(H \rightarrow gg) = \frac{M_H^3}{8\pi v^2} \left(\frac{\alpha_s}{\pi}\right)^2 n^2 |D(n)|^2 \quad (1.52)$$

We can plot now our results to see what we are dealing with. Here we see the branching ratios for the different Higgs decay channels analyzed till now:

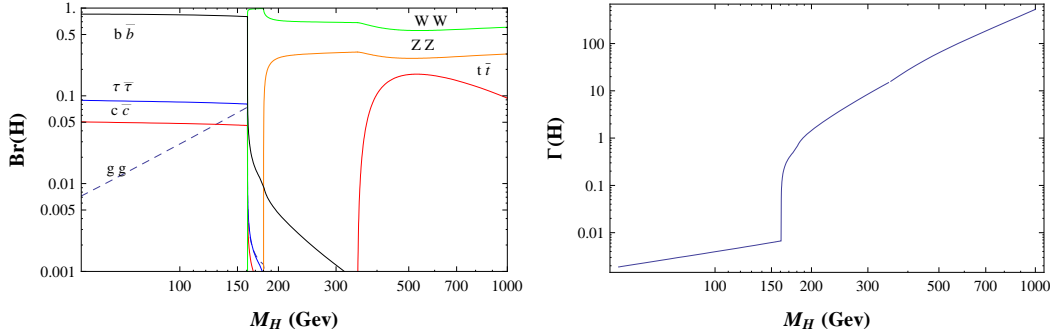


Figure 6: Higgs branching fractions (left) and Higgs decay rate (right) as functions of  $M_H$  without including 3-body decays.

Obviously, this doesn't look very good. In order to have a better vision of the Higgs decay to weak bosons we need to also include three body Higgs decays, that is, to one real and one virtual weak boson with the virtual boson decaying to anything. The first process that we shall consider is  $H \rightarrow WW^*$ ,  $W^* \rightarrow f_u f_d$  (where  $f_u = u, c, t, e, \mu, \tau$  and  $f_d = d, s, b, \nu_e, \nu_\mu, \nu_\tau$ ). Using this notation we do not distinguish between quarks and anti-quarks;  $f_u$  can be either an up quark or an anti-up quark depending if  $W$  is  $W^+$  or  $W^-$ . The only quark that is heavy enough to make an important contribution due to its mass it's the top quark, therefore it will be the only one that we shall not consider as massless. Thus, we have the following:

$$H(p_1) \rightarrow W^-(p_2)W^{*+}, W^{*+} \rightarrow t(p_3)\bar{b}(p_4)$$

The amplitude that we find for this process is:

$$\mathcal{M}_{(H \rightarrow Wtb)}^{(1)} = \frac{2M_W^2}{v} \epsilon_{r_2}^\mu \left( -g_{\mu\nu} + \frac{k_\mu k_\nu}{M_W^2} \right) \frac{1}{k^2 - M_W^2} \frac{g}{2\sqrt{2}} V_{tb} \bar{u}_t^{r_3} \gamma^\nu (1 - \gamma_5) v_b^{r_4} \quad (1.53)$$

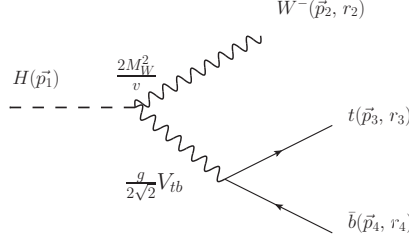


Figure 7: Three body Higgs decay, first contribution to  $H \rightarrow Wqq$ .

where  $\mathbf{k} = \mathbf{p}_3 + \mathbf{p}_4$ . It's hermitical conjugate is:

$$\mathcal{M}_{(H \rightarrow Wtb)}^{(1)\dagger} = \frac{2M_W^2}{v} \epsilon_{r_2}^{\alpha*} \left( -g_{\alpha\beta} + \frac{k_\alpha k_\beta}{M_W^2} \right) \frac{1}{k^2 - M_W^2} \frac{g}{2\sqrt{2}} V_{tb}^* \bar{v}_b^{r_4} \gamma^\beta (1 - \gamma_5) u_t^{r_3} \quad (1.54)$$

Thus, the squared transition amplitude of the process is given by:

$$\begin{aligned} \sum_{r_i} |\mathcal{M}_{(H \rightarrow Wtb)}^{(1)}|^2 &= g^2 \frac{M_W^4}{2v^2} |V_{tb}|^2 \left( -g^{\alpha\mu} + \frac{p_2^\alpha p_2^\mu}{M_W^2} \right) \left( -g_{\mu\nu} + \frac{k_\mu k_\nu}{M_W^2} \right) \left( -g_{\alpha\beta} + \frac{k_\alpha k_\beta}{M_W^2} \right) \\ &\quad \frac{1}{[k^2 - M_W^2]^2} Tr\{ (p_3 + m_t) \gamma^\nu (1 - \gamma_5) p_4 \gamma^\beta (1 - \gamma_5) \} \end{aligned} \quad (1.55)$$

We shall break down the calculation of the amplitude in two pieces. The first piece is the spinor trace:

$$\begin{aligned} T^{\beta\nu} &\equiv Tr\{ (p_3 + m_t) \gamma^\nu (1 - \gamma_5) p_4 \gamma^\beta (1 - \gamma_5) \} \\ &= 8(i\epsilon^{\beta\nu\rho\sigma} p_{3\rho} p_{4\sigma} + p_4^\beta p_3^\nu + p_3^\beta p_4^\nu - g^{\beta\nu} p_3 p_4) \end{aligned} \quad (1.56)$$

The second piece that we have is:

$$\begin{aligned} G_{\beta\nu} &\equiv \left( -g^{\alpha\mu} + \frac{p_2^\alpha p_2^\mu}{M_W^2} \right) \left( -g_{\mu\nu} + \frac{k_\mu k_\nu}{M_W^2} \right) \left( -g_{\alpha\beta} + \frac{k_\alpha k_\beta}{M_W^2} \right) \\ &= -g_{\beta\nu} + \frac{1}{M_W^2} (2k_\beta k_\nu + p_{2\beta} p_{2\nu}) + \frac{1}{M_W^6} [(kp_2)^2 k_\beta k_\nu] - \frac{1}{M_W^4} [kp_2(p_{2\beta} k_\nu + k_\beta p_{2\nu}) + k^2 k_\beta k_\nu] \end{aligned} \quad (1.57)$$

with:

$$p_3^2 = m_t^2 = m^2; \quad p_4^2 = m_b^2 \approx 0; \quad kp_3 = m^2 + p_3 p_4; \quad kp_4 = p_3 p_4 \quad (1.58)$$

Now we will define the Lorentz invariant kinematical variables:

$$\begin{aligned} s_{23} &\equiv (p_2 + p_3)^2 = M_W^2 + m^2 + 2p_2 p_3; \quad s_{24} \equiv (p_2 + p_4)^2 = M_W^2 + 2p_2 p_4 \\ s_{34} &\equiv (p_3 + p_4)^2 = m^2 + 2p_3 p_4 \end{aligned} \quad (1.59)$$

These 3 variables are not independent. They satisfy:

$$s_{23} + s_{24} + s_{34} = M_H^2 + M_W^2 + m^2 \quad (1.60)$$

In order to be able to express  $T^{\beta\nu} G_{\beta\nu}$  as a function of  $s_{ij}$  and the three masses we will need the following expressions:

$$p_2 p_3 = \frac{1}{2}(M_H^2 - s_{24} - s_{34}); \quad p_2 p_4 = \frac{1}{2}(s_{24} - M_W^2); \quad p_3 p_4 = \frac{1}{2}(s_{34} - m^2) \quad (1.61)$$

Thus, we can express  $T^{\beta\nu}G_{\beta\nu}$  in the Lorentz invariant form:

$$\begin{aligned}
T^{\beta\nu}G_{\beta\nu} &= -8m^2 - 4M_H^2 + 4s_{24} + 8s_{34} - \frac{m^2}{M_W^6}(m^2 - s_{34})(M_H^2 - s_{34})^2 \\
&+ \frac{1}{M_W^2} \left( -9m^4 + m^2(4s_{24} + 5s_{34} + 4M_H^2) - 4s_{24}(s_{24} + s_{34} - M_H^2) \right) \\
&+ \frac{2m^2}{M_W^4} \left( m^2(M_H^2 + s_{34}) + s_{34}(2s_{24} - s_{34}) - M_H^2(2s_{24} + s_{34}) \right)
\end{aligned} \tag{1.62}$$

And the amplitude for this process is:

$$\sum_{r_i} |\mathcal{M}_{(H \rightarrow Wtb)}^{(1)}|^2 = g^2 \frac{M_W^4}{2v^2} |V_{tb}|^2 \frac{1}{[s_{34} - M_W^2]^2} G^{\beta\nu} T_{\beta\nu} \tag{1.63}$$

The second process that we need to include here is:

$$H(p_1) \rightarrow W^+(p_2)W^{*-}, W^{*-} \rightarrow \bar{t}(p_3)b(p_4)$$

The squared amplitude of this process brings the same contribution as the one before, therefore, we find that:

$$\sum_{r_i} |\mathcal{M}_{(H \rightarrow Wtb)}|^2 = g^2 \frac{M_W^4}{v^2} |V_{tb}|^2 \frac{1}{[s_{34} - M_W^2]^2} G^{\beta\nu} T_{\beta\nu} \tag{1.64}$$

So the decay width of this process is given by the formula:

$$\Gamma(H \rightarrow Wtb) = N_C \frac{g^2}{2v^2} \frac{M_W^4}{M_H} |V_{tb}|^2 \int dQ_3 \frac{G^{\beta\nu} T_{\beta\nu}}{[s_{34} - M_W^2]^2} \tag{1.65}$$

We must consider now the Lorentz invariant three body phase space ( $1 \rightarrow 2, 3, 4$ ):

$$d^2Q_3 = \frac{1}{128\pi^3 s} ds_{34} ds_{24} \tag{1.66}$$

with  $s \equiv (p_2 + p_3 + p_4)^2 = M_H^2$  and the following kinematical restrictions:

$$(m_2 + m_4)^2 \leq s_{24} \leq (\sqrt{s} - m_3)^2; \quad s_{34}^{min} \leq s_{34} \leq s_{34}^{max} \tag{1.67}$$

where  $s_{34}^{min}$  and  $s_{34}^{max}$  are given by:

$$\begin{aligned}
s_{34}^{min} &= \frac{1}{4s_{24}} \left[ (s - m_2^2 - m_3^2 + m_4^2)^2 - (\lambda^{1/2}(s, s_{24}, m_3^2) + \lambda^{1/2}(s_{24}, m_2^2, m_4^2))^2 \right] \\
s_{34}^{max} &= \frac{1}{4s_{24}} \left[ (s - m_2^2 - m_3^2 + m_4^2)^2 - (\lambda^{1/2}(s, s_{24}, m_3^2) - \lambda^{1/2}(s_{24}, m_2^2, m_4^2))^2 \right]
\end{aligned} \tag{1.68}$$

Applied to our configuration we have:

$$\begin{aligned}
s_{34}^{min} &= \frac{1}{4s_{24}} \left[ (M_H^2 - M_W^2 - m^2)^2 - (\lambda^{1/2}(M_H^2, s_{24}, m^2) + \lambda^{1/2}(s_{24}, M_W^2, 0))^2 \right] \\
s_{34}^{max} &= \frac{1}{4s_{24}} \left[ (M_H^2 - M_W^2 - m^2)^2 - (\lambda^{1/2}(M_H^2, s_{24}, m^2) - \lambda^{1/2}(s_{24}, M_W^2, 0))^2 \right]
\end{aligned} \tag{1.69}$$

and of course:

$$M_W^2 \leq s_{24} \leq (M_H - m)^2 \tag{1.70}$$

We shall integrate the differential decay width numerically at the end of this section, when plotting the Higgs different branching ratios as functions of the Higgs mass.

The next process that we will consider is important for a **low mass Higgs**; it is the same process as the one before but with low mass fermions:

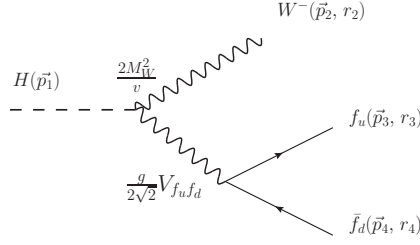


Figure 8: Three body Higgs decay, second contribution to  $H \rightarrow W q\bar{q}$ .

Here  $f_u = u, c, e, \mu, \tau$  and  $f_d = d, s, \nu_e, \nu_\mu, \nu_\tau$ . Neglecting all fermion masses we find that:

$$\Gamma(H \rightarrow W f_u f_d) = \frac{g^2}{2v^2} \frac{M_W^4}{M_H} \left( 3 + N_C \sum_{q_u, q_d} |V_{q_u q_d}|^2 \right) \int dQ_3 \frac{G'^{\beta\nu} T'_{\beta\nu}}{[s_{34} - M_W^2]^2} \quad (1.71)$$

with a simpler expression for the tensorial contraction:

$$G'^{\beta\nu} T'_{\beta\nu} = -4M_H^2 + 4s_{24} + 8s_{34} - \frac{4s_{24}}{M_W^2} (s_{24} + s_{34} - M_H^2) \quad (1.72)$$

In this case we have:

$$s_{34}^{max} = M_H^2 + M_W^2 - s_{24} - \frac{M_H^2 M_W^2}{s_{24}}; \quad s_{34}^{min} = 0; \quad M_W^2 \leq s_{24} \leq M_H^2 \quad (1.73)$$

Integrating with these limits, and introducing the notation  $x \equiv M_W^2/M_H^2$  we obtain the following :

$$\int dQ_3 \frac{G'^{\beta\nu} T'_{\beta\nu}}{[s_{34} - M_W^2]^2} = \frac{1}{384\pi^3 x} S(x) \quad (1.74)$$

with  $S(x)$  being:

$$S(x) = 47x^2 - 60x + 15 - \frac{2}{x} - 3(4x^2 - 6x + 1) \ln(x) - \frac{6(20x^2 - 8x + 1)}{(4x - 1)^{1/2}} \arccos\left(\frac{3x - 1}{2x^{3/2}}\right) \quad (1.75)$$

So we finally obtain, for massless fermions (all except the top quark):

$$\Gamma(H \rightarrow W f_u f_d) = \frac{g^2}{v^2} \frac{3M_W^2}{256\pi^3} M_H S(x) \quad (1.76)$$

The next process that we will be concerned with is a Higgs decay in a real and a virtual Z boson. We shall consider, as in the previous section, a massive top quark and all other fermions as massless. So the first process is:

$$H(p_1) \rightarrow Z(p_2)Z^*, Z^* \rightarrow t(p_3)\bar{t}(p_4)$$

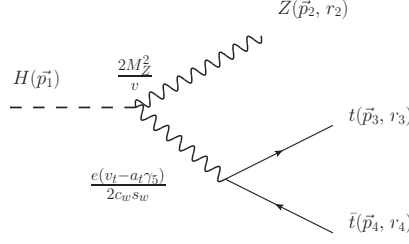


Figure 9: Three body Higgs decay, first contribution to  $H \rightarrow Zqq$ .

where  $s_w \equiv \sin\theta_w$  and  $c_w \equiv \cos\theta_w$  with  $\theta_w$  the weak mixing angle;  $v_t = \frac{1}{2} - \frac{4}{3}s_w^2$  and  $a_f = \frac{1}{2}$ . We have the following amplitude for this process:

$$\mathcal{M}_{(H \rightarrow Zt\bar{t})} = \frac{M_Z^2}{v} \frac{e}{c_w s_w} \epsilon_{r_2}^\mu \left( -g_{\mu\nu} + \frac{k_\mu k_\nu}{M_Z^2} \right) \frac{1}{k^2 - M_Z^2} \bar{u}_t^{r_3} \gamma^\nu (v_t - a_t \gamma_5) v_t^{r_4} \quad (1.77)$$

where  $\mathbf{k} = \mathbf{p}_3 + \mathbf{p}_4$ . It's hermitical conjugate is:

$$\mathcal{M}_{(H \rightarrow Zt\bar{t})}^\dagger = \frac{M_Z^2}{v} \frac{e}{c_w s_w} \epsilon_{r_2}^{\alpha*} \left( -g_{\alpha\beta} + \frac{k_\alpha k_\beta}{M_Z^2} \right) \frac{1}{k^2 - M_Z^2} \bar{v}_t^{r_4} \gamma^\beta (v_t - a_t \gamma_5) u_t^{r_3} \quad (1.78)$$

Therefore we find that:

$$\sum_{r_i} |\mathcal{M}_{(H \rightarrow Zt\bar{t})}|^2 = \frac{M_Z^4}{v^2} \frac{e^2}{c_w^2 s_w^2} \frac{T^{\beta\nu} G_{\beta\nu}}{[k^2 - M_Z^2]^2} \quad (1.79)$$

with the tensor  $G_{\beta\nu}$  the same as in the W case, changing of course,  $M_W$  with  $M_Z$  and with  $T^{\beta\nu}$  given by ( $m \equiv m_t$ ):

$$T^{\beta\nu} = \text{Tr}\{\gamma^\beta (v_t - a_t \gamma_5)(\not{p}_3 + m)\gamma^\nu (v_t - a_t \gamma_5)(\not{p}_4 - m)\} \quad (1.80)$$

Calculating the tensor contraction  $T^{\beta\nu} G_{\beta\nu}$ , introducing the kinematical variables  $s_{ij}$  and defining  $x \equiv M_Z^2/M_H^2$ ,  $y \equiv m^2/M_H^2$  we obtain:

$$\begin{aligned} T^{\beta\nu} G_{\beta\nu} = & -\frac{1}{2M_H^4 x^3} (((4(9y+1)x^3 + 3y(3y-4)x^2 - 2(y-2)yx + y^2)M_H^6 \\ & - (s_{34}(8x^3 + (15x+2)yx + 2(x+1)y^2 + 3y) + 4s_{24}x(x(x+y+1) - y))M_H^4 \\ & + (y(10x+y+6)s_{34}^2 + 4s_{24}x(x-y)s_{34} + 4s_{24}^2 x^2)M_H^2 - 3s_{34}^3 y)a^2 \\ & + v^2((4(1-5y)x^3 + y(9y+4)x^2 - 2y(y+2)x + y^2)M_H^6 \\ & + (s_{34}(-8x^3 + (5x+6)yx - 2(x+1)y^2 + y) - 4s_{24}x(x(x+y+1) - y))M_H^4 \\ & + (4s_{24}(s_{24} + s_{34})x^2 + s_{34}^2 y^2 - 2s_{34}(3xs_{34} + s_{34} + 2s_{24}x)y)M_H^2 + s_{34}^3 y)) \end{aligned} \quad (1.81)$$

We shall also integrate this result numerically when plotting the Higgs branching ratios. For a low mass Higgs contribution we consider all other fermions as massless, therefore in the previous result we need to set  $y = 0$ , we finally obtain:

$$T'^{\beta\nu} G'_{\beta\nu} = -\frac{1}{M_H^2 x} 2(a_f^2 + v_f^2)(xM_H^4 - (xs_{24} + s_{24} + 2s_{34}x)M_H^2 + s_{24}(s_{24} + s_{34}))$$

where  $f = u, d, c, s, b, e, \mu, \tau, \nu_e, \nu_\mu, \nu_\tau$ . Integrating over the same interval as in the W case we obtain:

$$\int dQ_3 \frac{G'^{\beta\nu} T'_{\beta\nu}}{[s_{34} - M_Z^2]^2} = \frac{1}{768\pi^3 x} S(x) \quad (1.82)$$

with  $S(x)$  being the same as before. We finally obtain, for massless fermions (all except the top quark):

$$\Gamma(H \rightarrow Z f \bar{f}) = \frac{e^2}{c_w^2 s_w^2} \frac{M_Z^2}{1536 v^2 \pi^3} M_H S(x) \sum_f (a_f^2 + v_f^2) \quad (1.83)$$

We have the following values of  $v_f$  and  $a_f$ :

	$u_j$	$d_j$	$\nu_l$	1
$v_f$	$\frac{1}{2} - \frac{4}{3} \sin^2 \theta_w$	$-\frac{1}{2} + \frac{2}{3} \sin^2 \theta_w$	$\frac{1}{2}$	$-\frac{1}{2} + 2 \sin^2 \theta_w$
$a_f$	$\frac{1}{2}$	$-\frac{1}{2}$	$\frac{1}{2}$	$-\frac{1}{2}$

Therefore, performing the sum, we obtain:

$$\begin{aligned} \sum_f (a_f^2 + v_f^2) &= N_C \sum_{j=u,c} (a_j^2 + v_j^2) + N_C \sum_{j=d,s,b} (a_j^2 + v_j^2) + 3(a_l^2 + v_l^2) + 3(a_{\nu_l}^2 + v_{\nu_l}^2) \\ &= 3(2(a_u^2 + v_u^2) + 3(a_d^2 + v_d^2) + (a_l^2 + v_l^2) + (a_{\nu_l}^2 + v_{\nu_l}^2)) \\ &= 3\left(\frac{7}{2} - \frac{20}{3} \sin^2 \theta_w + \frac{80}{9} \sin^4 \theta_w\right) \\ &= 18\left(\frac{7}{12} - \frac{10}{9} \sin^2 \theta_w + \frac{40}{27} \sin^4 \theta_w\right) \\ &\equiv 18 R(\theta_w) \end{aligned} \quad (1.84)$$

Thus we find the following decay width:

$$\Gamma(H \rightarrow Z f \bar{f}) = \frac{g^2}{v^2} \frac{3M_Z^2}{256 \pi^3} M_H S(x) \frac{R(\theta_w)}{\cos^2 \theta_w} \quad (1.85)$$

Let's plot again the Higgs branching ratios including the three body decays described earlier and also the total Higgs decay width as a function of  $M_H$ :

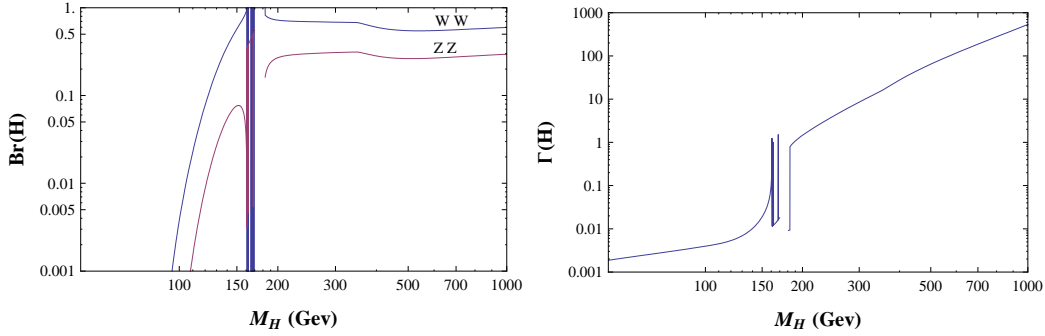


Figure 10: Higgs branching fractions (left) and Higgs decay rate (right) as functions of  $M_H$  including 3-body decays without including higher order corrections to the W/Z propagator.

As expected they behave badly close to the W and Z on-shell region. Therefore we need to include higher order corrections in order to eliminate the apparently singular behaviour. As we shall prove later, all we need to do, as a first order approximation, is to include the W/Z total decay width in the W/Z propagator as it follows:

$$\left(-g^{\mu\nu} + \frac{k^\mu k^\nu}{M_{W/Z}^2}\right) \frac{1}{k^2 - M_{W/Z}^2 + i\sqrt{s} \Gamma_{W/Z}(s)} \quad (1.86)$$

We have the following decay widths for the W and the Z boson for massless fermions:

$$\begin{aligned} \Gamma_W &= \frac{3g^2}{16\pi} M_W \quad \Rightarrow \quad \Gamma_W(s) = \frac{3g^2}{16\pi} \sqrt{s} \\ \Gamma_Z &= \frac{3R(\theta_w)g^2}{8\pi \cos^2 \theta_w} M_Z \quad \Rightarrow \quad \Gamma_Z(s) = \frac{3R(\theta_w)g^2}{8\pi \cos^2 \theta_w} \sqrt{s} \end{aligned} \quad (1.87)$$

Besides this correction for the propagators we shall also include in the Branching Ratios plot the two channels that we have ignored until now,  $H \rightarrow \gamma\gamma$  and  $H \rightarrow \gamma Z$  [16]. These processes also take place through loop diagrams, but they have much smaller decay rates because of the e.m. coupling constant ( $\alpha \ll \alpha_S$ ).

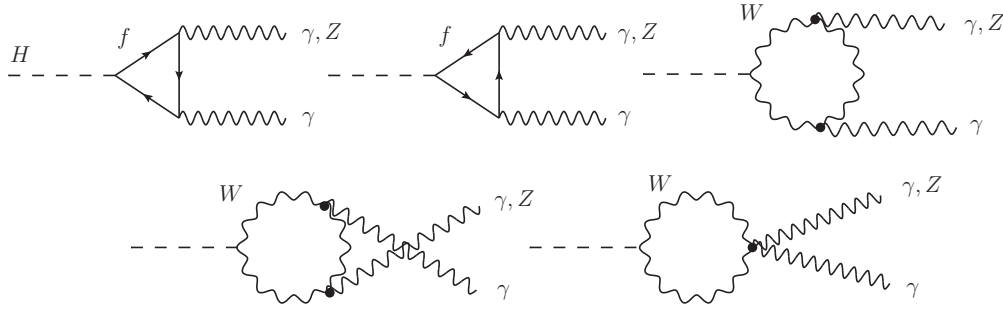


Figure 11: Diagrams that contribute to the  $H \rightarrow \gamma\gamma$  and to  $H \rightarrow \gamma Z$  processes.

Thus, putting it all together we find the following:

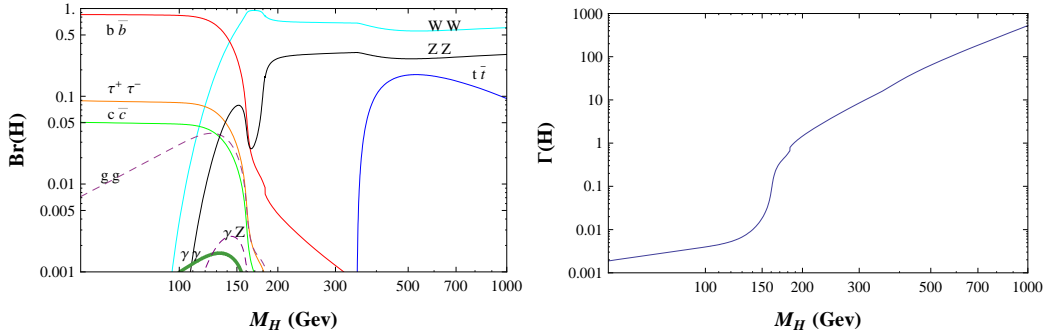


Figure 12: Higgs branching fractions (left) and Higgs decay rate (right) as functions of  $M_H$  including 3-body decays including higher order corrections to the W/Z propagator.

In order to get an even more precise result we would still need to include higher order QCD and EW corrections. The  $H \rightarrow \gamma Z$  and  $H \rightarrow \gamma\gamma$  have very small decay width as we mentioned earlier. We can observe here that for a low mass Higgs the dominating decay channel is  $H \rightarrow b\bar{b}$  whereas for a high mass Higgs, the  $H \rightarrow WW, ZZ$  are the dominating ones. Also, as we mentioned before, the  $H \rightarrow t\bar{t}$  channel brings important contributions due to the top quark large mass. We can also observe that the total decay width increases with the Higgs mass. This process becomes very strong above the  $H \rightarrow WW$  production threshold. By the time  $M_H$  reaches 800-1000 GeV it's decay rate becomes very broad, same size or bigger than it's mass. A direct measure of the Higgs couplings will be necessary if a Higgs particle is discovered. It would be necessary to detect it's decay into several decay channels in order to check if the coupling strength is proportional to the mass for all massive particles as the standard model predicts. This is probably an even more difficult task for a Higgs hunter than the actual discovery of a Higgs boson.

## 2 Higgs Main Production Channels

We are now in position to analyze three of the most important Higgs production channels at the LHC, gluon-gluon fusion, weak boson fusion and Higgs-strahlung. We shall start here with the first one, by computing the transition amplitude of the process  $gg \rightarrow H$  through a top triangle loop and afterwards we will integrate the cross section with the PDFs. The same will be done for the second and third channel.

### 2.1 Gluon-Gluon Fusion

$g(p_1)g(p_2) \rightarrow H(p_3)$ :

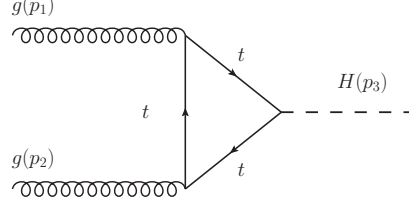


Figure 13: Gluon-gluon fusion process.

Obviously, this is the same amplitude as in the previous section. Let's see how the one particle phase space looks like:

$$\int dQ_1 = 2\pi \int \frac{d^3 p}{2E} \delta^{(4)}(\mathcal{P}_i - \mathcal{P}_f) = 2\pi \delta(s - M_H^2) \quad (2.1)$$

Therefore we easily find that:

$$\sigma(gg \rightarrow H) = \frac{\pi^2}{8M_H} \Gamma(H \rightarrow gg) \delta(s - M_H^2) = \frac{M_H^2}{64 v^2} \left( \frac{\alpha_s^2}{\pi} \right) n^2 |D(n)|^2 \delta(s - M_H^2) \quad (2.2)$$

with  $n^2 = m^4/M_H^4$ . Now we move to the next section and calculate the cross section for the next channel.

### 2.2 Weak Boson Fusion

$q(p_1)q(p_2) \rightarrow q(p_3)q(p_4)H(k)$ :

We have two contributions, one from Z bosons and another one from W bosons. The first one that we analyze is the W boson fusion which can be achieved in a couple of ways:

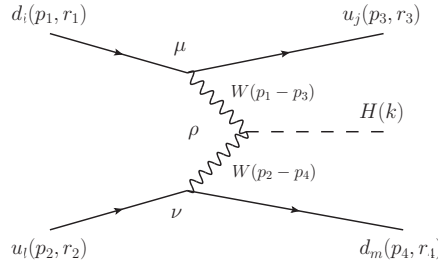


Figure 14: W boson fusion process, first contribution to  $qq \rightarrow qqH$ .

The amplitude we get is:

$$\mathcal{M} = \frac{2M_W^2 g^2}{v} V_{ij} V_{lm} \left( -g_\mu^\rho + \frac{k_{1\mu} k_1^\rho}{M_W^2} \right) \left( -g_{\nu\rho} + \frac{k_{2\nu} k_{2\rho}}{M_W^2} \right) \frac{\bar{u}_{r_4} \Gamma^\nu u_{r_2} \bar{u}_{r_3} \Gamma^\mu u_{r_1}}{(k_1^2 - M_W^2)(k_2^2 - M_W^2)} \quad (2.3)$$

Where we have defined the following:

$$k_1 \equiv p_1 - p_3; \quad k_2 \equiv p_2 - p_4; \quad \Gamma^\mu \equiv \gamma^\mu(1 - \gamma_5) \quad (2.4)$$

Calculating the tensor contraction of the two propagators:

$$\mathcal{M} = \frac{2M_W^2 g^2}{v} V_{ij} V_{lm} \left( g_{\mu\nu} - \frac{k_{1\mu} k_{1\nu} + k_{2\mu} k_{2\nu}}{M_W^2} + \frac{k_{1\mu} k_{2\nu} (k_1 k_2)}{M_W^4} \right) \frac{\bar{u}_{r_4} \Gamma^\nu u_{r_2} \bar{u}_{r_3} \Gamma^\mu u_{r_1}}{(k_1^2 - M_W^2)(k_2^2 - M_W^2)} \quad (2.5)$$

It's hermitical conjugate gives:

$$\mathcal{M}^\dagger = \frac{2M_W^2 g^2}{v} V_{ij}^* V_{lm}^* \left( g_{\alpha\beta} - \frac{k_{1\alpha} k_{1\beta} + k_{2\alpha} k_{2\beta}}{M_W^2} + \frac{k_{1\alpha} k_{2\beta} (k_1 k_2)}{M_W^4} \right) \frac{\bar{u}_{r_1} \Gamma^\alpha u_{r_3} \bar{u}_{r_2} \Gamma^\beta u_{r_4}}{(k_1^2 - M_W^2)(k_2^2 - M_W^2)} \quad (2.6)$$

In order to keep the notation simple we define the following quantities:

$$b \equiv \frac{2M_W^2 g^2}{v}; \quad D^{ij} \equiv (k_i^2 - M_W^2)(k_j^2 - M_W^2); \quad T_{\alpha\beta}^{ij} \equiv \left( g_{\alpha\beta} - \frac{k_{i\alpha} k_{i\beta} + k_{j\alpha} k_{j\beta}}{M_W^2} + \frac{k_{i\alpha} k_{j\beta} (k_i k_j)}{M_W^4} \right) \quad (2.7)$$

Therefore, with this new notation we have:

$$\mathcal{M} = \frac{b}{D^{12}} V_{ij} V_{lm} T_{\mu\nu}^{12} \bar{u}_{r_4} \Gamma^\nu u_{r_2} \bar{u}_{r_3} \Gamma^\mu u_{r_1}; \quad \mathcal{M}^\dagger = \frac{b}{D^{12}} V_{ij}^* V_{lm}^* T_{\alpha\beta}^{12} \bar{u}_{r_1} \Gamma^\alpha u_{r_3} \bar{u}_{r_2} \Gamma^\beta u_{r_4} \quad (2.8)$$

The squared averaged transition amplitude that we obtain is:

$$\overline{|\mathcal{M}|^2} \equiv \frac{N_C^2}{4 N_C^2} \sum_{r_i} |\mathcal{M}_{(1)}|^2 = \frac{b^2}{4(D^{12})^2} |V_{ij}|^2 |V_{lm}|^2 T_{\mu\nu}^{12} T_{\alpha\beta}^{12} G^{\alpha\mu\beta\nu} \quad (2.9)$$

Where we have defined:

$$G^{\alpha\mu\beta\nu} \equiv Tr\{\Gamma^\alpha p_3^\mu \Gamma^\mu p_1\} Tr\{\Gamma^\beta p_4^\nu \Gamma^\nu p_2\} \quad (2.10)$$

Calculating the spinor trace and the remaining tensor contraction we find:

$$G^{\alpha\mu\beta\nu} = 64(-i\epsilon^{\alpha\mu\gamma\rho} p_{1,\gamma} p_{3,\rho} + p_3^\alpha p_1^\mu + p_1^\alpha p_3^\mu - g^{\alpha\mu} (p_1 p_3)) (-i\epsilon^{\beta\nu\tau\xi} p_{2,\tau} p_{4,\xi} + p_4^\beta p_2^\nu + p_2^\beta p_4^\nu - g^{\beta\nu} (p_2 p_4))$$

$$T_{\mu\nu}^{12} T_{\alpha\beta}^{12} G^{\alpha\mu\beta\nu} = 256(p_1 \cdot p_2)(p_3 \cdot p_4) \quad (2.11)$$

The final expression for the squared matrix amplitude is:

$$\overline{|\mathcal{M}_{d_i u_l \rightarrow u_j d_m H}|^2} = \frac{64 M_W^8}{v^6} |V_{ij}|^2 |V_{lm}|^2 \frac{(p_1 \cdot p_2)(p_3 \cdot p_4)}{[(p_1 - p_3)^2 - M_W^2]^2 [(p_2 - p_4)^2 - M_W^2]^2} \quad (2.12)$$

The next diagram that we can include here is:

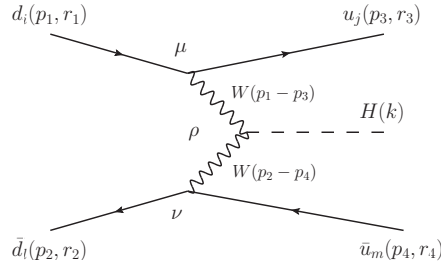


Figure 15: W boson fusion process, second contribution to  $qq \rightarrow qqH$ .

In order to obtain this amplitude we only have to change the spinor trace for:

$$G^{\prime\alpha\mu\beta\nu} = \sum_{r_i} \bar{u}_{r_1} \Gamma^\alpha u_{r_3} \bar{v}_{r_4} \Gamma^\beta u_{r_2} \bar{u}_{r_2} \Gamma^\nu v_{r_4} \bar{u}_{r_3} \Gamma^\mu u_{r_1} = \text{Tr}\{\Gamma^\alpha \not{p}_3 \Gamma^\mu \not{p}_1\} \text{Tr}\{\Gamma^\beta \not{p}_2 \Gamma^\nu \not{p}_4\} \quad (2.13)$$

Calculating the spinor trace we obtain:

$$G^{\prime\alpha\mu\beta\nu} = 64(-i\epsilon^{\alpha\mu\gamma\rho} p_{1,\gamma} p_{3,\rho} + p_3^\alpha p_1^\mu + p_1^\alpha p_3^\mu - g^{\alpha\mu}(p_1 p_3)) \times \\ (+i\epsilon^{\beta\nu\tau\xi} p_{2,\tau} p_{4,\xi} + p_4^\beta p_2^\nu + p_2^\beta p_4^\nu - g^{\beta\nu}(p_2 p_4)) \quad (2.14)$$

The tensor contraction then gives:

$$T_{\mu\nu}^{12} T_{\alpha\beta}^{12} G^{\prime\alpha\mu\beta\nu} = 256(p_1 \cdot p_4)(p_2 \cdot p_3) \quad (2.15)$$

Thus, in this case we find a similar cross section:

$$\overline{|\mathcal{M}_{d_i \bar{d}_i \rightarrow u_j \bar{u}_m H}|^2} = \frac{64 M_W^8}{v^6} |V_{ij}|^2 |V_{lm}|^2 \frac{(p_1 \cdot p_4)(p_2 \cdot p_3)}{[(p_1 - p_3)^2 - M_W^2]^2 [(p_2 - p_4)^2 - M_W^2]^2} \quad (2.16)$$

We now analyze the diagrams corresponding Z boson fusion. We shall see that for this process there are a lot more diagrams that contribute than the ones coming from W fusion. The interference between Z and W diagrams is less than 1 %, so we can neglect it [16]. What we have left is:

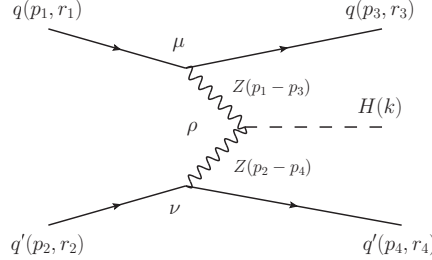


Figure 16: Z boson fusion process, third contribution to  $qq \rightarrow qqH$ .

The scattering amplitude and its hermitical conjugate is:

$$\mathcal{M} = \frac{2M_Z^2}{v} \frac{e^2}{4c^2\theta_w s^2\theta_w} \left(-g_\mu^\rho + \frac{k_{1\mu}k_1^\rho}{M_Z^2}\right) \left(-g_{\nu\rho} + \frac{k_{2\nu}k_{2\rho}}{M_Z^2}\right) \frac{\bar{u}_{r_4} \Gamma^\nu u_{r_3} \bar{u}_{r_3} \Gamma^\mu u_{r_1}}{(k_1^2 - M_Z^2)(k_2^2 - M_Z^2)} \\ \mathcal{M}^\dagger = \frac{2M_Z^2}{v} \frac{e^2}{4c^2\theta_w s^2\theta_w} \left(g_{\alpha\beta} - \frac{k_{1\alpha}k_{1\beta} + k_{2\alpha}k_{2\beta}}{M_Z^2} + \frac{k_{1\alpha}k_{2\beta}(k_1 k_2)}{M_Z^4}\right) \frac{\bar{u}_{r_1} \Gamma^\alpha u_{r_3} \bar{u}_{r_2} \Gamma^\beta u_{r_4}}{(k_1^2 - M_Z^2)(k_2^2 - M_Z^2)} \quad (2.17)$$

where we have defined

$$\Gamma^\mu \equiv \gamma^\mu(v_q - a_q \gamma_5); \quad \Gamma'^\beta \equiv \gamma^\beta(v_{q'} - a_{q'} \gamma_5) \quad (2.18)$$

We easily obtain the following result:

$$\overline{|\mathcal{M}_{qq' \rightarrow qq'H}|^2} = \frac{M_Z^4}{2v^2} \frac{e^4}{c^4\theta_w s^4\theta_w} \frac{(p_1 \cdot p_4)(p_2 \cdot p_3) \mathbf{C}_{\mathbf{q}\mathbf{q}'} + (p_1 \cdot p_2)(p_3 \cdot p_4) \mathbf{D}_{\mathbf{q}\mathbf{q}'}}{[(p_1 - p_3)^2 - M_W^2]^2 [(p_2 - p_4)^2 - M_W^2]^2} \quad (2.19)$$

with  $C_{qq'} = (a_{q'}^2 + v_{q'}^2)(a_q^2 + v_q^2) - 4a_q a_{q'} v_q v_{q'}$  and  $D_{qq'} = (a_{q'}^2 + v_{q'}^2)(a_q^2 + v_q^2) + 4a_q a_{q'} v_q v_{q'}$ .

The next contribution comes from the following process:

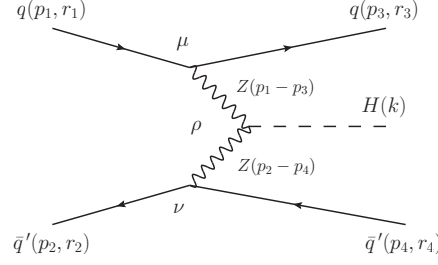


Figure 17: Z boson fusion process, fourth contribution to  $qq \rightarrow qqH$ .

with  $q \neq q'$ . Again, it's easy to find the squared transition amplitude for this process:

$$\overline{\sum} |\mathcal{M}_{q\bar{q}' \rightarrow q\bar{q}' H}|^2 = \frac{M_Z^4}{2v^2} \frac{e^4}{c^4 \theta_w s^4 \theta_w} \frac{(p_1 \cdot p_4)(p_2 \cdot p_3) \mathbf{D}_{\mathbf{q}\mathbf{q}'} + (p_1 \cdot p_2)(p_3 \cdot p_4) \mathbf{C}_{\mathbf{q}\mathbf{q}'}}{[(p_1 - p_3)^2 - M_W^2]^2 [(p_2 - p_4)^2 - M_W^2]^2} \quad (2.20)$$

If  $q = q'$  we have an additional diagram that contributes to the process:

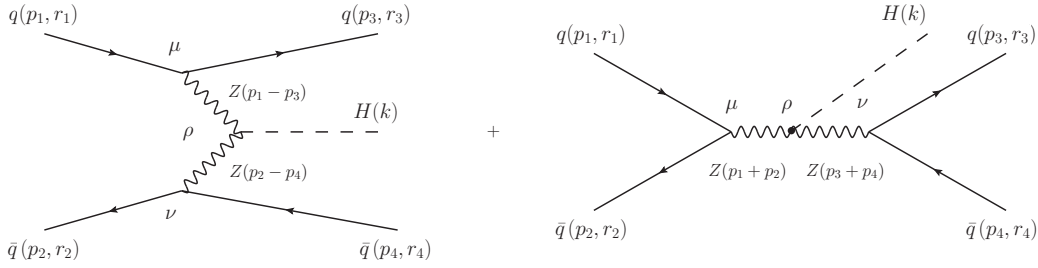


Figure 18: Z boson fusion process, fifth and sixth contributions to  $qq \rightarrow qqH$ .

The first diagram is easy to compute by setting  $v_q = v'_q$  and  $a_q = a'_q$  for the last process:

$$\overline{\sum} |\mathcal{M}_{(1)}|^2 = \frac{M_Z^4}{2v^2} \frac{e^4}{c^4 \theta_w s^4 \theta_w} \frac{(p_1 \cdot p_4)(p_2 \cdot p_3) (a_q^4 + 6v_q^2 a_q^2 + v_q^4) + (p_1 \cdot p_2)(p_3 \cdot p_4) (a_q^2 - v_q^2)^2}{[(p_1 - p_3)^2 - M_W^2]^2 [(p_2 - p_4)^2 - M_W^2]^2} \quad (2.21)$$

The second diagram gives the following contribution:

$$\begin{aligned} \mathcal{M}_{(2)} &= \frac{2M_Z^2}{v} \frac{e^2}{4c^2 \theta_w s^2 \theta_w} \left( -g_\mu^\rho + \frac{k'_{1\mu} k'_{1\rho}}{M_Z^2} \right) \left( -g_{\nu\rho} + \frac{k'_{2\nu} k'_{2\rho}}{M_Z^2} \right) \frac{\bar{v}_{r_2} \Gamma^\mu u_{r_1} \bar{u}_{r_3} \Gamma^\nu v_{r_4}}{[(p_1 + p_2)^2 - M_Z^2] [(p_3 + p_4)^2 - M_Z^2]} \\ \mathcal{M}_{(2)}^\dagger &= \frac{2M_Z^2}{v} \frac{e^2}{4c^2 \theta_w s^2 \theta_w} \left( -g_\alpha^\rho + \frac{k'_{1\alpha} k'_{1\rho}}{M_Z^2} \right) \left( -g_{\beta\rho} + \frac{k'_{2\beta} k'_{2\rho}}{M_Z^2} \right) \frac{\bar{v}_{r_4} \Gamma^\beta u_{r_3} \bar{u}_{r_1} \Gamma^\alpha v_{r_2}}{[(p_1 + p_2)^2 - M_Z^2] [(p_3 + p_4)^2 - M_Z^2]} \end{aligned} \quad (2.22)$$

where we have defined  $k'_1 = p_1 + p_2$  and  $k'_2 = p_3 + p_4$ . The squared amplitude of the second diagram, therefore, reads:

$$\overline{\sum} |\mathcal{M}_{(2)}|^2 = \frac{M_Z^4}{2v^2} \frac{e^4}{c^4 \theta_w s^4 \theta_w} \frac{(p_1 \cdot p_4)(p_2 \cdot p_3) (a_q^4 + 6v_q^2 a_q^2 + v_q^4) + (p_1 \cdot p_3)(p_2 \cdot p_4) (a_q^2 - v_q^2)^2}{[(p_1 + p_2)^2 - M_W^2]^2 [(p_3 + p_4)^2 - M_W^2]^2} \quad (2.23)$$

We shall not write down the contribution coming from the crossed term because it's a very large term. In order to compute this term we would need numerical integration procedures for the three body phase space and also for the convolution with the PDFs. We shall use the data from [18, 19] in order to plot the Weak-Boson Fusion cross section in the next section.

There is another process that also contributes to this production channel that we need to include in our discussion:

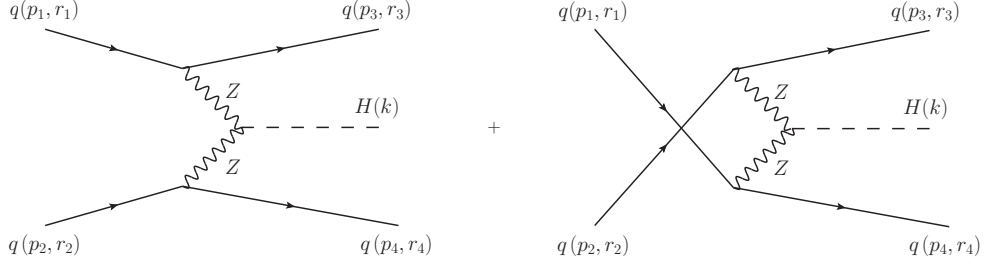


Figure 19: Z boson fusion process, last two contributions to  $qq \rightarrow qqH$ .

Again, these diagrams have the same problem with a very large cross term. We move on now and calculate the cross section for the next Higgs production channel.

### 2.3 Higgs-strahlung

$\bar{q}(p_1)q(p_2) \rightarrow H(p_3) W, Z(p_4)$ :

The first process that we shall analyze is the one corresponding to a Z boson production and a radiated Higgs:

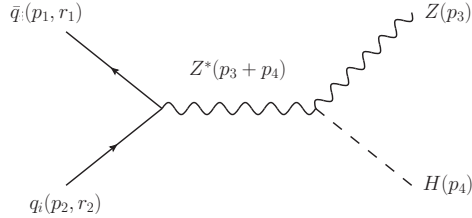


Figure 20: Higgs-strahlung, first diagram.

defining  $k \equiv p_1 + p_2 = p_3 + p_4$ , the scattering amplitude that we find for this first process and it's hermitical conjugate read:

$$\begin{aligned} \mathcal{M}_{\bar{q}_i q_i \rightarrow HZ} &= \frac{2M_Z^2}{v} \frac{e}{2c_{\theta_w} s_{\theta_w}} \epsilon_{r_3}^\nu \bar{v}_{r_1} \gamma^\mu (v_{q_i} - a_{q_i} \gamma_5) u_{r_2} \left( -g_{\mu\nu} + \frac{k_\mu k_\nu}{M_Z^2} \right) \frac{1}{k^2 - M_Z^2} \\ \mathcal{M}_{\bar{q}_i q_i \rightarrow HZ}^\dagger &= \frac{2M_Z^2}{v} \frac{e}{2c_{\theta_w} s_{\theta_w}} \epsilon_{r_3}^{\beta*} \bar{u}_{r_2} \gamma^\alpha (v_{q_i} - a_{q_i} \gamma_5) v_{r_1} \left( -g_{\alpha\beta} + \frac{k_\alpha k_\beta}{M_Z^2} \right) \frac{1}{k^2 - M_Z^2} \end{aligned} \quad (2.24)$$

Therefore we find the following squared transition matrix:

$$\begin{aligned} \sum_{r_1, r_2} |\mathcal{M}_{\bar{q}_i q_i \rightarrow HZ}|^2 &= \frac{e^2 M_Z^4}{v^2 c_{\theta_w}^2 s_{\theta_w}^2} \epsilon_{r_3}^{\beta*} \epsilon_{r_3}^\nu \left( -g_{\mu\nu} + \frac{k_\mu k_\nu}{M_Z^2} \right) \left( -g_{\alpha\beta} + \frac{k_\alpha k_\beta}{M_Z^2} \right) \\ &\quad \frac{1}{[k^2 - M_Z^2]^2} \text{Tr} \{ \gamma^\alpha (v_{q_i} - a_{q_i} \gamma_5) \not{p}_1 \gamma^\mu (v_{q_i} - a_{q_i} \gamma_5) \not{p}_2 \} \end{aligned} \quad (2.25)$$

Calculating the spinorial trace and performing the tensor contraction we obtain the simple result:

$$\overline{|\mathcal{M}_{\bar{q}_i q_i \rightarrow HZ}|^2} \equiv \frac{1}{4N_C^2} \sum_{r_i} N_C |\mathcal{M}_{\bar{q}_i q_i \rightarrow HZ}|^2 = \frac{1}{N_C} \frac{e^2 M_Z^2}{v^2 c_{\theta_w}^2 s_{\theta_w}^2} \frac{a_{q_i}^2 + v_{q_i}^2}{[k^2 - M_Z^2]^2} (p_1 p_2 M_Z^2 + 2(p_1 p_3)(p_2 p_3)) \quad (2.26)$$

In the partonic center of mass frame we have the following:

$$p_1^\mu = (p, \vec{p}); \quad p_2^\mu = (p, -\vec{p}); \quad p_3^\mu = (E_Z, \vec{p}'); \quad p_4^\mu = (E_H, -\vec{p}'). \quad (2.27)$$

Therefore we find the following results:

$$\begin{aligned} \rightarrow p_1 p_2 &= 2p^2 = s/2; \quad p_1 p_3 = pE_Z - \vec{p}\vec{p}' = pE_Z - pp' \cos \theta; \quad p_2 p_3 = pE_Z + \vec{p}\vec{p}' = pE_Z + pp' \cos \theta. \\ \rightarrow 2(p_1 p_3)(p_2 p_3) &= 2(p^2 E_Z^2 - p^2 p'^2 \cos^2 \theta) = 2p^2 (M_Z^2 + p'^2 - p'^2 \cos^2 \theta) = 2p^2 (M_Z^2 + p'^2 \sin^2 \theta) \\ \rightarrow p_1 p_2 M_Z^2 + 2(p_1 p_3)(p_2 p_3) &= \frac{sM_Z^2}{2} + \frac{s}{2} (M_Z^2 + p'^2 \sin^2 \theta) = sM_Z^2 + \frac{s}{2} p'^2 \sin^2 \theta \end{aligned} \quad (2.28)$$

The 2-body phase space does not depend on  $\phi$  thus:

$$dQ_2 = \frac{1}{2\pi} \frac{p'}{4\sqrt{s}} d\cos\theta \quad (2.29)$$

Integrating we obtain:

$$\int dQ_2 (p_1 p_2 M_Z^2 + 2(p_1 p_3)(p_2 p_3)) = \frac{s p'}{4\pi\sqrt{s}} (M_Z^2 + \frac{1}{3} p'^2) \quad (2.30)$$

Knowing that  $p'$  can be written as  $p' = \lambda^{1/2}(s, M_Z^2, M_H^2)/(2\sqrt{s})$  and doing all the simplifications we get to the following:

$$\sigma(\bar{q}_i q_i \rightarrow HZ) = \frac{M_Z^4 \lambda^{1/2}(s, M_Z^2, M_H^2)}{144 \pi s^2 v^4} \frac{\lambda(s, M_Z^2, M_H^2) + 12s M_Z^2}{[s - M_Z^2]^2} (a_{q_i}^2 + v_{q_i}^2) \quad (2.31)$$

The second process that we shall analyze corresponds to a  $W^+$  boson production and a radiated Higgs:

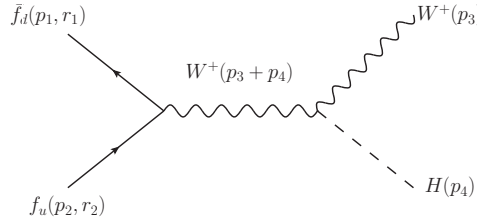


Figure 21: Higgs-strahlung, second diagram.

Here we have defined  $k \equiv p_1 + p_2 = p_3 + p_4$  and  $f_u = u, c$ ,  $f_d = d, s, b$  massless as in the previous sections; the scattering amplitude that we find for this first process and it's hermitical conjugate read:

$$\begin{aligned} \mathcal{M}_{\bar{f}_d f_u \rightarrow HW^+} &= \frac{2M_W^2}{v} \frac{g}{2\sqrt{2}} \epsilon_{r_3}^\nu \bar{v}_{r_1} \gamma^\mu (1 - \gamma_5) u_{r_2} \left( -g_{\mu\nu} + \frac{k_\mu k_\nu}{M_W^2} \right) \frac{V_{\bar{f}_d f_u}}{k^2 - M_W^2} \\ \mathcal{M}_{\bar{f}_d f_u \rightarrow HW^+}^\dagger &= \frac{2M_W^2}{v} \frac{g}{2\sqrt{2}} \epsilon_{r_3}^{\beta*} \bar{u}_{r_2} \gamma^\alpha (1 - \gamma_5) v_{r_1} \left( -g_{\alpha\beta} + \frac{k_\alpha k_\beta}{M_W^2} \right) \frac{V_{\bar{f}_d f_u}^*}{k^2 - M_W^2} \end{aligned} \quad (2.32)$$

Therefore we find the following squared transition matrix:

$$\begin{aligned} \sum_{r_1, r_2} |\mathcal{M}_{\bar{f}_d f_u \rightarrow HW^+}|^2 &= \frac{g^2 M_W^4}{2v^2} \epsilon_{r_3}^{\beta*} \epsilon_{r_3}^\nu \left( -g_{\mu\nu} + \frac{k_\mu k_\nu}{M_W^2} \right) \left( -g_{\alpha\beta} + \frac{k_\alpha k_\beta}{M_W^2} \right) \\ &\quad \frac{|V_{\bar{f}_d f_u}|^2}{[k^2 - M_W^2]^2} Tr\{\gamma^\alpha (1 - \gamma_5) \not{p}_1 \gamma^\mu (1 - \gamma_5) \not{p}_2\} \end{aligned} \quad (2.33)$$

Again, calculating the spinorial trace and performing the tensor contraction we obtain a simple result:

$$\overline{\sum} |\mathcal{M}_{\bar{f}_d f_u \rightarrow HW^+}|^2 \equiv \frac{1}{4N_C^2} \sum_{r_i} N_C |\mathcal{M}_{\bar{f}_d f_u \rightarrow HW^+}|^2 = \frac{1}{N_C} \frac{g^2 M_W^2}{v^2} \frac{|V_{\bar{f}_d f_u}|^2}{[k^2 - M_W^2]^2} (p_1 p_2 M_W^2 + 2(p_1 p_3)(p_2 p_3)) \quad (2.34)$$

In the partonic center of mass frame we have the same as before; the only thing we need to do is substitute  $M_Z$  for  $M_W$ . Therefore we obtain the following cross section:

$$\sigma(\bar{f}_d f_u \rightarrow HW^+) = \frac{M_W^4 \lambda^{1/2}(s, M_W^2, M_H^2)}{144 \pi s^2 v^4} \frac{\lambda(s, M_W^2, M_H^2) + 12s M_W^2}{[s - M_W^2]^2} |V_{\bar{f}_d f_u}|^2 \quad (2.35)$$

The second process that contributes to a W production corresponds to a  $W^-$  and a radiated Higgs giving the same contribution as the one calculated before for a  $W^+$ . The total cross section is then given by:

$$\sigma(\bar{q}_i q_j \rightarrow HW) = \sigma(\bar{f}_d f_u \rightarrow HW^+) + \sigma(f_d \bar{f}_u \rightarrow HW^-) = 2\sigma(f_d \bar{f}_u \rightarrow HW^-) = 2\sigma(\bar{f}_d f_u \rightarrow HW^+) \quad (2.36)$$

## 2.4 Parton Distribution Functions and Integrated Cross Sections

The basic assumption of the partonic model is that all known hadrons are composed by partons, point-like particles which can be quarks or gluons. For example, as we all know, a proton, at low energies appears to be made out of two up quarks and one down quark which we shall call the valence quarks. However, deep inelastic scattering experiments show that at higher energies, besides the valence quarks, we can find other quarks, antiquarks and gluons inside the proton. This can be easily interpreted; at high enough energies any virtual gluon can become a quark-antiquark pair:

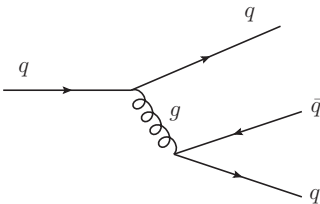


Figure 22: Pair production by a virtual gluon inside a proton.

This gives rise to the parton distribution functions which are scale dependent. Using the **MSTW** PDFs database (<http://projects.hepforge.org/mstwpdf/>) we can make the following example plots (Fig. 23) for  $\mu^2 = 10 \text{ GeV}^2$  and  $\mu^2 = 10^4 \text{ GeV}^2$  hadronic center of mass energy at NNLO, with  $\mu$  being the PDFs energy scale, also known as the factorization scale. If we also wish to include the errors then we obtain Fig. 24. Note that our plots are slightly different from the ones found in the **MSTW** website, and it is because they use different confidence levels (the 68% CL instead of 95% CL sets that we use). The PDFs scale that we are going to use here is  $\mu = M_H$  which goes from 100 GeV to 1000 TeV. Another interesting thing that we should learn here is that there is no top quark inside a proton at these energy scales; that is why in previous scattering processes like ( $q q' \rightarrow \text{anything}$ ) we have never considered a possible top quark. The plot from Fig. 25 shows the top and bottom PDFs as a function of the momentum fraction  $\mathbf{x}$  and the scale  $\mu$ .

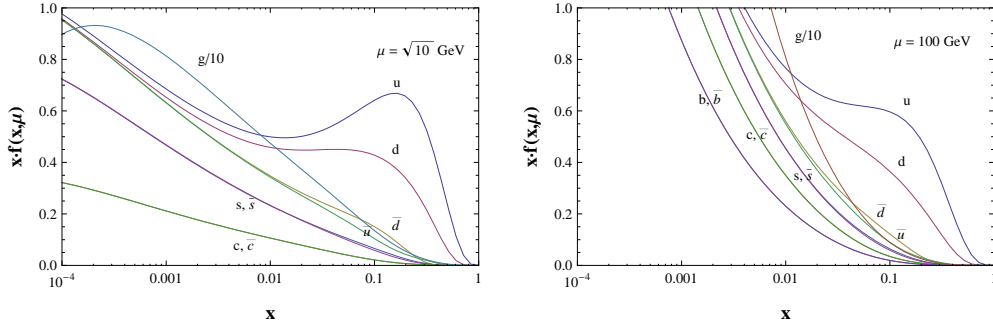


Figure 23: Parton Distribution Functions at two energy scales without including errors.

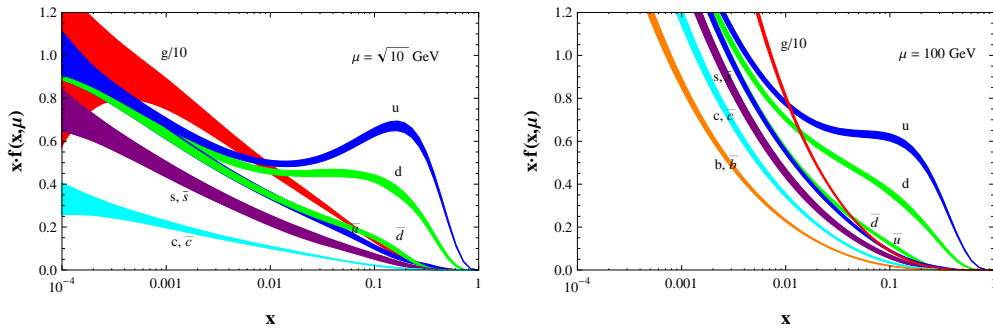


Figure 24: Parton Distribution Functions including errors.

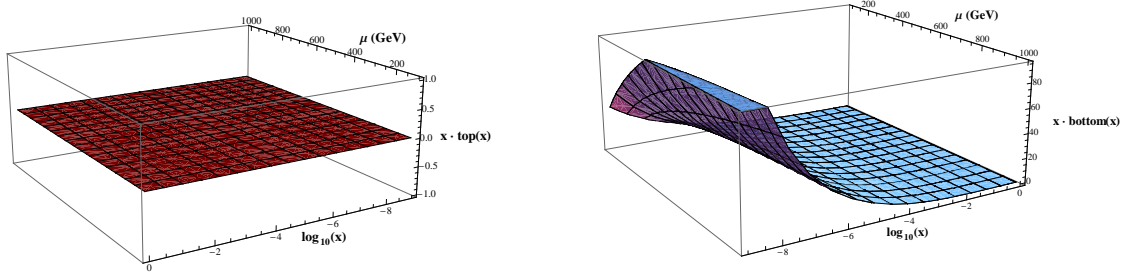


Figure 25: Top (left) and bottom (right) distribution functions as functions of  $M_H$  and the energy scale  $\mu$ .

The first process that we shall convolute with the PDF's is the **gluon-gluon fusion** process. In the hadronic center of mass the process can be visualised like this:

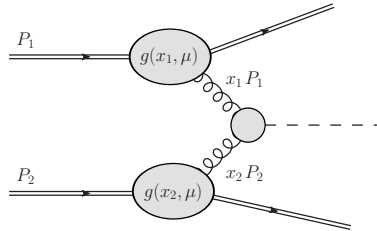


Figure 26: Partonic model of the gluon-gluon scattering process.

The two colliding protons carry momenta  $P_1$  and  $P_2$ , thus, a gluon from the first proton with momentum  $p_{g_1} = x_1 P_1$  is scattered by another gluon with momentum  $p_{g_2} = x_2 P_2$  from the second proton.  $x_1$  and  $x_2$  are called momentum fractions and  $0 \leq x_{1,2} \leq 1$ ;  $g(x_i, \mu)$  are the parton distribution functions for the gluons. They represent the probability density of finding a gluon with momentum  $p_{g_i}$  inside a proton that carries a momentum  $P_i$  at a energy scale  $\mu$ . Let's relate now the parton center of mass frame (PCM) with the hadronic center of mass (HCM). We are going to plot the cross section for very high HCM energies so we can consider the proton as massless. Therefore in the HCM frame we can write:

$$P_1^\mu = (p, -\vec{p}); \quad P_2^\mu = (p, \vec{p}) \quad \Rightarrow \quad S = (P_1 + P_2)^2 = 2P_1 P_2 = 4p^2 \quad (2.37)$$

Thus we can easily relate  $s$  with  $S$ :

$$s = (p_{g_1} + p_{g_2})^2 = (x_1 P_1 + x_2 P_2)^2 = x_1 x_2 S \equiv \tau S \quad (2.38)$$

Let us also define the following quantity:  $\tau_0 \equiv M_H^2/S$ . Let's also remember how the cross section in the PCM frame looked like (from now on we shall write all the cross sections calculated in the PCM as  $\hat{\sigma}$ ):

$$\hat{\sigma}(gg \rightarrow H) = \frac{M_H^2}{64v^2} \left( \frac{\alpha_s^2}{\pi} \right) n^2 |D(n)|^2 \delta(s - M_H^2) \quad (2.39)$$

Let's express the Dirac delta function in terms of  $x_1$ ,  $x_2$  and  $\tau_0$ :

$$\delta(s - M_H^2) = \delta(x_1 x_2 S - M_H^2) = \delta(x_1 S (x_2 - \frac{M_H^2}{x_1 S})) = \frac{1}{x_1 S} \delta(x_2 - \frac{\tau_0}{x_1}) \quad (2.40)$$

The total integrated cross section is given by the expression:

$$\begin{aligned} \sigma(gg \rightarrow H) &= \int dx_1 \int dx_2 g(x_1, \mu) g(x_2, \mu) \hat{\sigma}(gg \rightarrow H) \\ &= \frac{n^2}{64v^2} \left( \frac{\alpha_s^2}{\pi} \right) |D(n)|^2 \int dx_1 \int dx_2 g(x_1, \mu) g(x_2, \mu) \frac{\tau_0}{x_1} \delta(x_2 - \frac{\tau_0}{x_1}) \\ &= \frac{n^2 \tau_0}{64v^2} \left( \frac{\alpha_s^2}{\pi} \right) |D(n)|^2 \int_{\tau_0}^1 \frac{dx_1}{x_1} g(x_1, \mu) g(\tau_0/x_1, \mu) \end{aligned} \quad (2.41)$$

This cross section is to be integrated numerically. The following plot shows the dependence of  $\sigma(gg \rightarrow H)$  with the Higgs mass at three different HCM energies,  $\sqrt{S} = 1.96$ , 7 and 14 TeV. As expected, the LHC cross section at  $\sqrt{S}=14$  TeV is the dominating one. It reaches  $\sigma \approx 30$  pb for a 100 GeV Higgs mass. The cross section at  $\sqrt{S} = 7$  TeV is approximately three times lower and finally the one corresponding to the Tevatron energy is very low, more than one order of magnitude smaller. The bump in the cross section is originated by the imaginary part of  $D(n)$  which becomes non-zero at  $M_H = 2m_t$ .

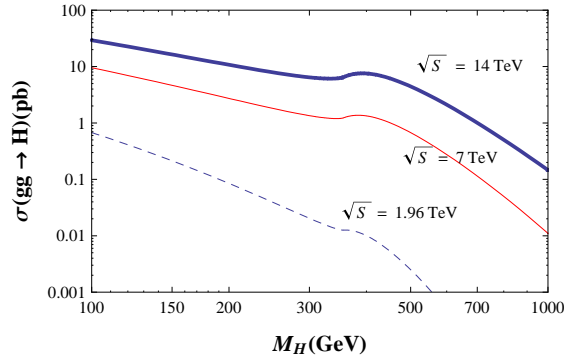


Figure 27: Gluon-gluon fusion cross section at  $\sqrt{S} = 7$  and 14 TeV for  $pp$  collisions at the LHC and at  $\sqrt{S} = 1.96$  TeV for  $p\bar{p}$  collisions at Tevatron.

The second process that we analyze is the **Higgs-strahlung** process. The total hadronic cross section for the HW case takes this form:

$$\begin{aligned} \sigma(\bar{q}q \rightarrow HW) &= \sum_{\bar{f}_d, f_u} \int_{\tau_0}^1 dx_1 \int_{\tau_0/x_1}^1 dx_2 \left( \bar{f}_d(x_1, \mu) f_u(x_2, \mu) + \bar{f}_d(x_2, \mu) f_u(x_1, \mu) \right) \hat{\sigma}(\bar{f}_d f_u, \rightarrow HW^+) \\ &+ \sum_{\bar{f}_u, f_d} \int_{\tau_0}^1 dx_1 \int_{\tau_0/x_1}^1 dx_2 \left( \bar{f}_u(x_1, \mu) f_d(x_2, \mu) + \bar{f}_u(x_2, \mu) f_d(x_1, \mu) \right) \hat{\sigma}(\bar{f}_u f_d, \rightarrow HW^-) \end{aligned} \quad (2.42)$$

with the kinematical restrictions  $\hat{\sigma}(s) = \hat{\sigma}(x_1 x_2 S)$  and  $\tau_0 = (M_H + M_W)^2/S$ . Integrating  $\hat{\sigma}$  for the same three different values of S as in the previous example, and plotting it as a function of  $M_H$  we find the following:

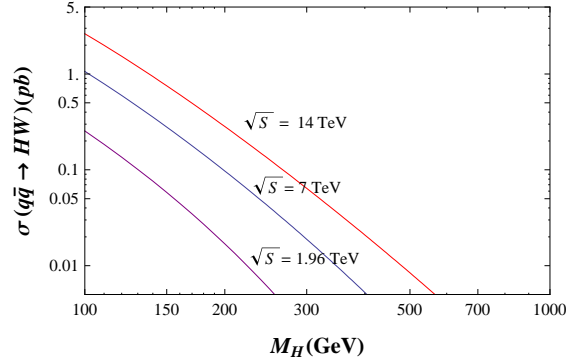


Figure 28:  $q\bar{q} \rightarrow WH$  cross section at  $\sqrt{S} = 7$  and 14 TeV for  $pp$  collisions at the LHC and at  $\sqrt{S} = 1.96$  TeV for  $p\bar{p}$  collisions at Tevatron.

As for the HZ process, we have the following:

$$\sigma(\bar{q}q \rightarrow HZ) = \sum_i \int_{\tau_0}^1 dx_1 \int_{\tau_0/x_1}^1 dx_2 \left( \bar{q}_i(x_1, \mu) q_i(x_2, \mu) + \bar{q}_i(x_2, \mu) q_i(x_1, \mu) \right) \hat{\sigma}(\bar{q}_i q_i, \rightarrow HZ) \quad (2.43)$$

We do the same plot for this cross section:

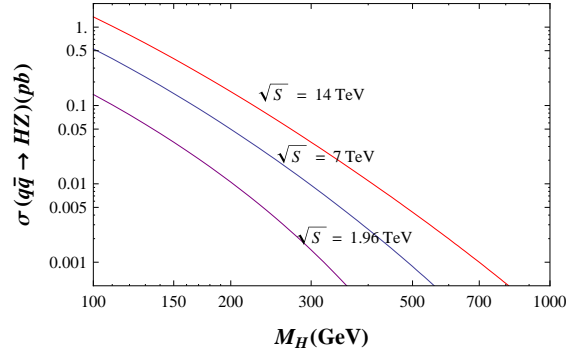


Figure 29:  $q\bar{q} \rightarrow ZH$  cross section at  $\sqrt{S} = 7$  and 14 TeV for  $pp$  collisions at the LHC and at  $\sqrt{S} = 1.96$  TeV for  $p\bar{p}$  collisions at Tevatron.

As we mentioned before, we shall also include here the Weak Boson Fusion integrated cross section at the same three different energies. Using [18, 19] we find the following cross sections:

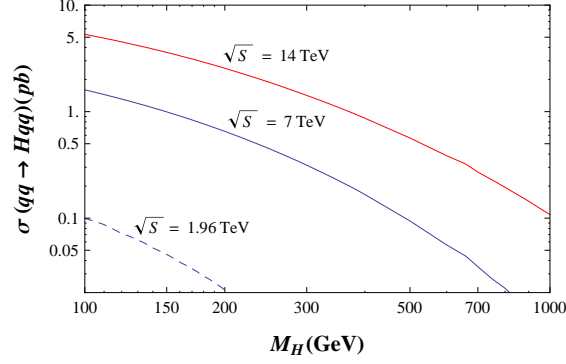


Figure 30:  $qq \rightarrow Hqq$  cross section at  $\sqrt{S} = 7$  and 14 TeV for  $pp$  collisions at the LHC and at  $\sqrt{S} = 1.96$  TeV for  $p\bar{p}$  collisions at Tevatron.

Therefore, we can now plot the cross sections as a function of the Higgs mass for the three different center of mass energies, 7 and 14 TeV for the LHC  $pp$  collision and 1.96 TeV for the Tevatron  $p\bar{p}$  collision. For the Tevatron at 1.96 TeV hadronic center of mass energy we find:

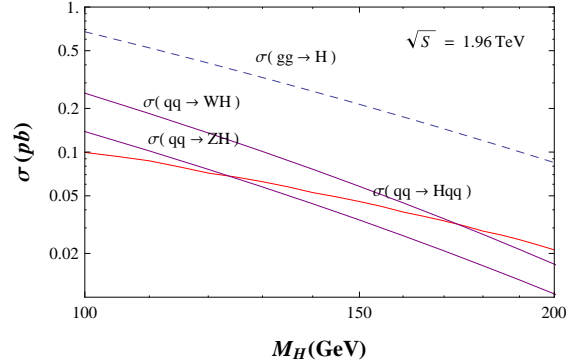


Figure 31: Tevatron main Higgs production channels at  $\sqrt{S} = 1.96$  TeV.

For the LHC at 7 and 14 TeV hadronic center of mass energy we find:

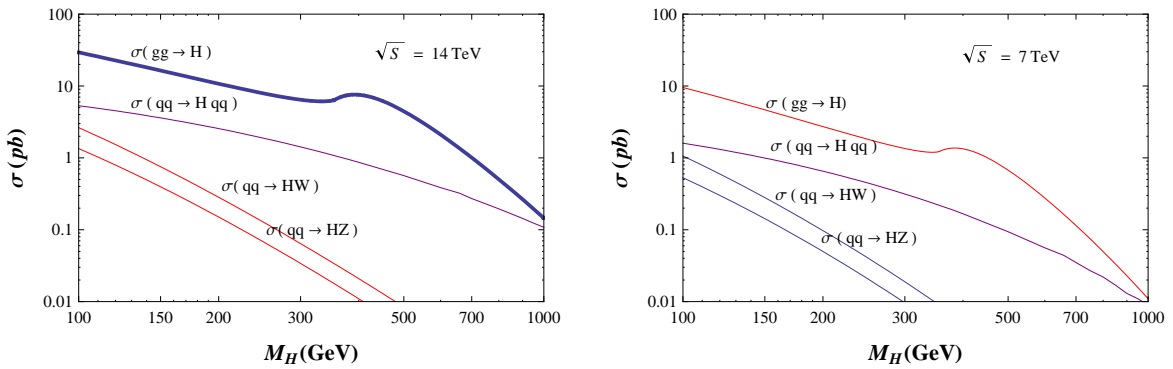


Figure 32: LHC main Higgs production channels at  $\sqrt{S} = 14$  TeV (left) and at  $\sqrt{S} = 7$  TeV (right).

We can see that in all three cases the dominating production channel is the gluon-gluon fusion. It is at least one order of magnitude higher than all the others. The distance between this channel and Higgs-strahlung channels gets higher as the Higgs mass increases. This is not the case for weak boson fusion channel.

At  $M_H \sim 700 - 1000$  GeV,  $gg \rightarrow H$  and  $qq \rightarrow W/Z H$  get very close. However, a SM Higgs mass this high is not so probable based on the latest electroweak precision fits that we shall talk about in section 4. A natural question now arises. Are these LO cross sections precise enough? How badly do they get modified by higher order QCD and EW corrections? Let's consider for instance the gluon fusion channel. At higher orders we find a lot more diagrams that contribute to the process (Fig.33).

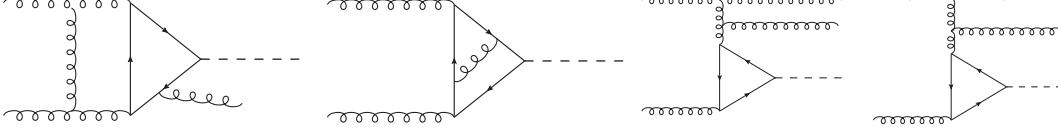


Figure 33: Some NLO and NNLO diagrams that contribute to the  $gg \rightarrow H$  process.

Contributions are known up to NNLO for QCD and NLO for EW theory. Using the data from [18] we can actually plot the cross section including these higher order corrections ( $\sigma_{HO}$ ) and compare it with our LO cross section ( $\sigma_{LO}$ ) at, for example,  $\sqrt{S} = 14$  TeV.

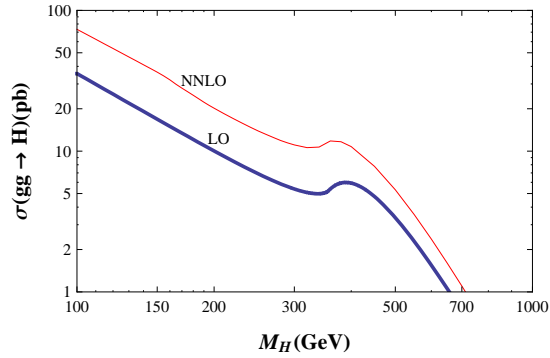


Figure 34: LO and NNLO  $gg \rightarrow H$  cross sections as functions of  $M_H$  at  $\sqrt{S} = 14$  TeV.

We can observe that  $\sigma_{HO}$  is  $\sim 3$  times bigger than  $\sigma_{LO}$ . In order to quantify the enhancement of the cross section due to higher order corrections it is usual to define the K-factor:  $K \equiv \sigma_{HO}/\sigma_{LO}$ . Therefore, K depends on  $M_H$  and is  $\sim 2-3$  at NNLO for the gluon fusion channel. As we can see, we need a good knowledge of this factor in order to give a precise prediction of the cross sections. We can take another example and see that in general this factor is very important and can be very peculiar. For the Higgs-strahlung channel we find [16]:

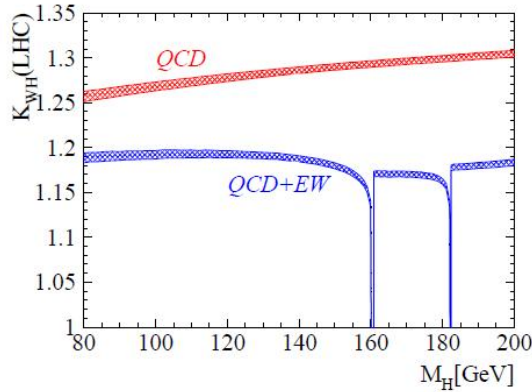


Figure 35: K - factor as function of  $M_H$  including NNLO QCD and NLO EW corrections.

So, not only is important to know the QCD corrections but also the EW ones. In this example, the NLO EW corrections change a little bit the behaviour of the K-factor; they reduce the enhancement produced by the NNLO QCD corrections and two peaks appear for the W and Z on-shell regions. If we ignore the two peaks the difference between them is less than 0.1. But the interesting fact is that these corrections can, at least partially, cancel each other (if we consider the fermionic contributions negative then the bosonic ones are positive, therefore a cancellation occurs). A comparison plot is shown below for all the channels discussed here.

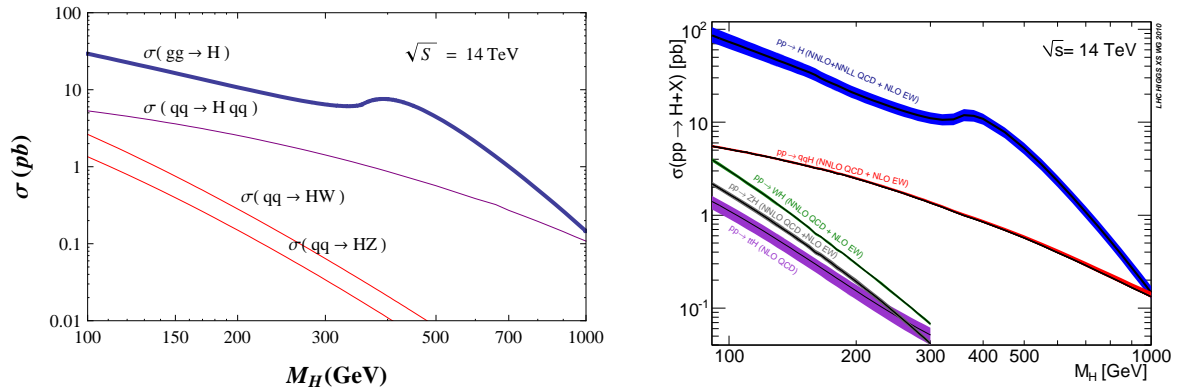


Figure 36: LHC main Higgs production channels at  $\sqrt{S} = 14$  TeV at LO (left) and including all known higher order corrections (right).

## 2.5 Fourth generation SM extension (SM4)

It has been experimentally established that there are at least three generations of leptons and quarks. This is, in fact, one of the basic assumptions of the SM. However, there is no reason to believe that there couldn't be more generations not yet discovered. The simplest model that includes a fourth generation is the extended Standard Model (SM4). Experiments like LHC and Tevatron are looking for fourth generation leptons. Until now there hasn't been found any trace of these new particles, therefore, this allows us to establish lower mass limits for the fermions [12, 13]:

$$m_{\nu_4} > 80.5 - 101.5 \text{ GeV}; \quad m_{l_4} > 100.8 \text{ GeV}; \quad m_{b_4} > 372 \text{ GeV}; \quad m_{t_4} > 335 \text{ GeV}.$$

An upper limit due to unitarity for  $t_4$  is close to 500 GeV, however, we are not interested in the upper limits here. We shall consider minimum  $t_4$  and  $b_4$  masses in order to see the minimum effect that produces the presence of the fourth generation in the SM. As we have seen in the previous section, the dominating Higgs production channel is by far the gluon-gluon fusion. Let's first see how this channel gets modified when we introduce a fourth generation quarks with their minimum masses:

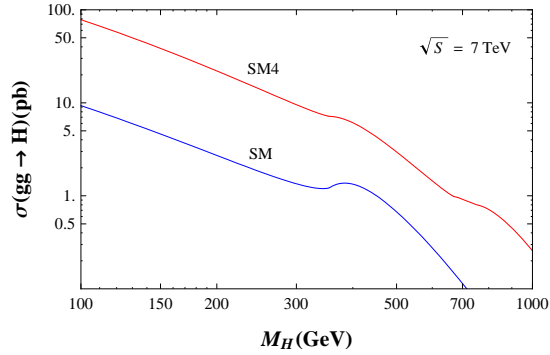


Figure 37: Gluon fusion cross section at  $\sqrt{S} = 7 \text{ TeV}$  for SM4 and SM as functions of  $M_H$ .

Because of the imaginary part of the form factor  $D(n)$  we now find three bumps in the cross section. This globally makes the  $\sigma_{SM4}$  become way bigger than the one predicted by the SM. Let's define the quotient  $R \equiv \sigma(gg \rightarrow H)_{SM4} / \sigma(gg \rightarrow H)_{SM}$  and plot it as a function of the Higgs mass. We obtain the following result:

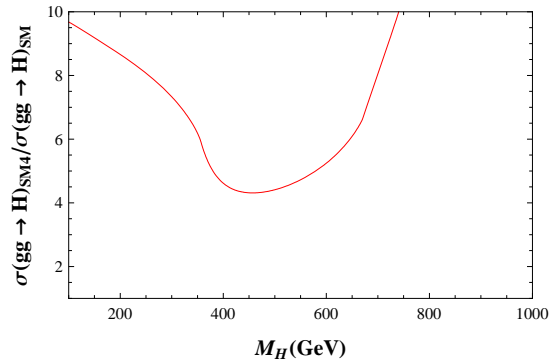


Figure 38: R quotient as a function of  $M_H$ .

We observe that it starts with a value of 9 approximately for 100 GeV Higgs mass, it reaches a minimum of about 4 for 400-500 GeV Higgs mass and afterwards it increases very rapidly. Let's compare this plot with the latest experimental results presented at the International Europhysics Conference on High Energy Physics in Grenoble, France, this year in July. If we take a look at the combined results on SM Higgs search with the CMS detector we find the following plot [15]:

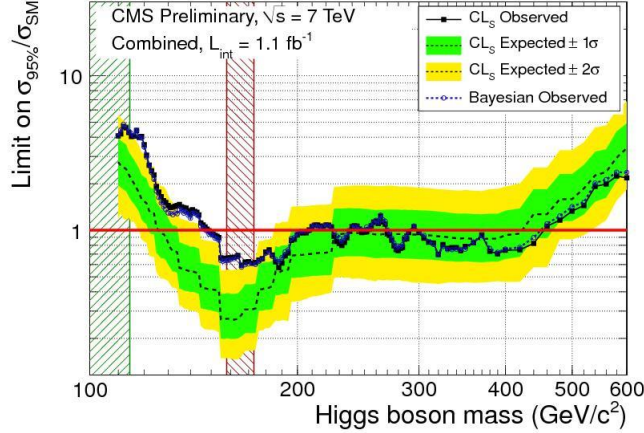


Figure 39: Experimental limit on  $\sigma_{95\%}/\sigma_{SM}$  as a function of  $M_H$  including statistical errors.

Here  $\sigma_{95\%}$  is the observed cross section with 95% confidence level. We can see that close to 100-110 GeV for the Higgs mass, it reaches values close to SM4 predictions so we can not draw any clear conclusion in that region. However, we can safely discard a fourth generation in the 120 - 600 GeV region. There the value of  $\sigma_{95\%}/\sigma_{SM}$  stays way lower than one, therefore it stays far away from the minimum value of the SM4 prediction, which is  $\approx 4$ . This next plot confirms our conclusion [15]:

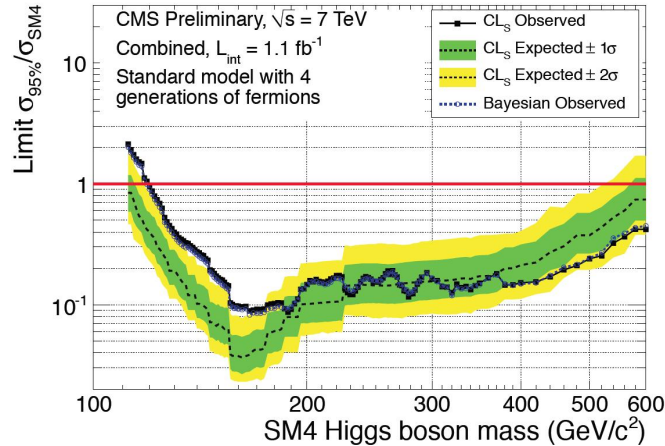


Figure 40: Experimental limit on  $\sigma_{95\%}/\sigma_{SM4}$  as a function of  $M_H$  including statistical errors.

Here we can see the quotient  $\sigma_{95\%}/\sigma_{SM4}$  as a function of  $M_H$ . We can see that in the region we mentioned above it stays below 1. Therefore we can safely exclude a fourth generation SM for a  $M_H$  in between 120 and 600 GeV.

### 3. Higgs Mass Renormalization

Let us consider only the pieces of the electroweak lagrangian that we wish to renormalize in terms of bare parameters. We have the following terms:

$$\begin{aligned} \mathcal{L}(x) = & \frac{1}{2} \partial_\mu H_0 \partial^\mu H_0 - \frac{1}{2} M_0^2 H_0^2 - \frac{M_0^2}{2v} H_0^3 + \mathcal{L}_W^{kin} + \mathcal{L}_Z^{kin} \\ & + \frac{2M_W^2}{v} W_\mu^\dagger W^\mu H_0 + \frac{M_Z^2}{v} Z_\mu Z^\mu H_0 - \frac{m}{v} H_0 \bar{f} f \end{aligned} \quad (3.1)$$

where the terms with index **0** are the bare parameters and the terms with the **kin** upper index are the kinetic terms corresponding to the W and Z fields. Note that the weak boson fields W and Z do not carry **0** index because here we are not considering their renormalization, but only the Higgs mass and field renormalization. Now let's consider the one-loop self-energy diagrams that will contribute to the Higgs field and mass renormalization:

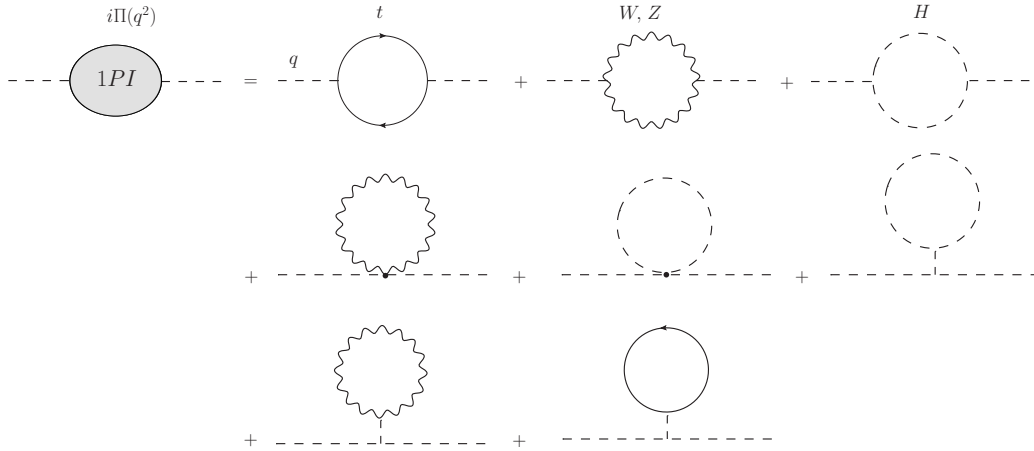


Figure 41: One particle irreducible (1PI) diagrams contributing to Higgs one loop renormalization.

This reads:

$$i\Pi(q^2) = i\Pi^{(t)}(q^2) + i\Pi^{(W_1)}(q^2) + i\Pi^{(Z_1)}(q^2) + i\Pi^{(H_1)}(q^2) + i\Pi^{(W_2)}(q^2) + i\Pi^{(Z_2)}(q^2) + \dots \quad (3.2)$$

We will be working in the unitary gauge, thus, we have no goldstone bosons besides the physical Higgs, nor ghosts to deal with. The one loop diagrams  $\Pi(q^2)$  can be split in two pieces, one that contains the Gamma pole  $1/\epsilon$  and another one that is free of ultraviolet divergences:

$$\Pi(q^2) = \Pi_\epsilon(\mu) + \Pi_R(q^2, \mu^2) \quad (3.3)$$

In order to renormalize the Higgs propagator we shall perform the Dyson summation of one particle irreducible (1PI) one-loop diagrams:



Figure 42: Renormalization using Dyson summation.

This reads:

$$\begin{aligned} iS(q^2) &= iS^{(0)}(q^2) + iS^{(0)}(q^2) i\Pi(q^2) iS^{(0)}(q^2) + \dots \\ S(q^2) &= S^{(0)}(q^2) - S^{(0)}(q^2) \Pi(q^2) S^{(0)}(q^2) + \dots \end{aligned} \quad (3.4)$$

Writing the scalar field propagators explicitly we have:

$$S(q^2) = \frac{1}{q^2 - M_0^2} - \frac{\Pi(q^2)}{[q^2 - M_0^2]^2} + \dots = \frac{1}{q^2 - M_0^2 + \Pi(q^2)} \quad (3.5)$$

We follow the standard procedure to relate the non-renormalized propagator  $S(q^2)$  with the renormalized one  $S_R(q^2)$ :

$$S(q^2) = \frac{1}{q^2 - M_0^2 + \Pi(q^2)} \equiv Z_1 S_R(q^2) = \frac{Z_1}{q^2 - M^2 + \Pi_R(q^2, \mu^2)} \quad (3.6)$$

$M$  is the renormalised Higgs mass and we define it the following way:

$$M^2 \equiv M_0^2 + \delta M^2 = Z_1 Z_2^{-1} M_0^2 \Rightarrow M_0^2 = Z_1^{-1} Z_2 M^2 \quad (3.7)$$

Using the relation between the T-ordered product and the propagator we find  $H_0 = Z_1^{1/2} H$ . Now we can write the initial lagrangian in terms of the renormalized quantities. We have the following:

$$\begin{aligned} \mathcal{L}(x) = & Z_1 \frac{1}{2} \partial_\mu H \partial^\mu H - Z_2 \frac{1}{2} M^2 H^2 - Z_2 Z_1^{1/2} \frac{M^2}{2v} H^3 + \mathcal{L}_W^{kin} + \mathcal{L}_Z^{kin} \\ & + Z_1^{1/2} \frac{2M_W^2}{v} W_\mu^\dagger W^\mu H + Z_1^{1/2} \frac{M_Z^2}{v} Z_\mu Z^\mu H + Z_1^{1/2} \frac{m}{v} H \bar{f} f \end{aligned} \quad (3.8)$$

This lagrangian is now expressed in terms of the renormalized physical parameters and is free of ultraviolet divergences. Therefore, in our Feynman diagrams we must switch the bare Higgs propagator with the renormalized one:

Let's take a closer look at the denominator:

$$\frac{i}{q^2 - M^2 + \Pi_R(q^2)} = \frac{i}{q^2 - M^2 + \text{Re}\{\Pi_R(q^2)\} + i \text{Im}\{\Pi_R(q^2)\}} \quad (3.9)$$

If we ignore, as a first order approximation, the real part of  $\Pi_R(q^2)$  then, what we have left is the imaginary part, which, carries away the propagator's pole from the real to the complex plane. If we refer to the cross section, this will be proportional to the squared complex modulus of the propagator, which, no longer goes to infinity nowhere in the real plane. Thus, only by computing the imaginary parts of the self-energy diagrams we obtain a well behaved, physical cross section. There is an easy way to obtain the imaginary part of  $i\Pi(q^2)$ , without having to calculate it explicitly, by using the Optical Theorem:

### 3.1 Optical Theorem:

We know that the scattering operator  $\mathcal{S}$  can be written as  $\mathcal{S} = \mathcal{I} - i\mathcal{M}$ , also that unitarity guarantees that  $\mathcal{S}^\dagger \mathcal{S} = \mathcal{I}$ . Therefore, we can write the following:

$$\mathcal{S}^\dagger \mathcal{S} = (\mathcal{I} + i\mathcal{M}^\dagger)(\mathcal{I} - i\mathcal{M}) = \mathcal{I} - i\mathcal{M} + i\mathcal{M}^\dagger + \mathcal{M}^\dagger \mathcal{M} \quad (3.10)$$

Thus, we obtain:

$$i(\mathcal{M} - \mathcal{M}^\dagger) = \mathcal{M}^\dagger \mathcal{M} \quad (3.11)$$

Now, let's analyze the transition between a initial state  $|i\rangle$  and a final state  $|f\rangle$ :

$$i\langle f|\mathcal{M} - \mathcal{M}^\dagger|i\rangle = \langle f|\mathcal{M}^\dagger \mathcal{M}|i\rangle \quad \text{with} \quad \langle f|\mathcal{M}|i\rangle = (2\pi)^4 \delta^{(4)}(\mathcal{P}_f - \mathcal{P}_i) \mathcal{M}_{i \rightarrow f} \quad (3.12)$$

If we introduce the closure relation in between  $\mathcal{M}^\dagger$  and  $\mathcal{M}$  we get:

$$i\langle f|\mathcal{M} - \mathcal{M}^\dagger|i\rangle = \widetilde{\sum}_n \langle f|\mathcal{M}^\dagger|n\rangle \langle n|\mathcal{M}|i\rangle \quad (3.13)$$

where  $|n\rangle$  is a complete basis of orthogonal states and  $\widetilde{\sum}_n$  is defined as:

$$\widetilde{\sum}_n \equiv \sum_n \frac{1}{(2\pi)^{3n_j}} \int \prod_{l=1}^{n_j} \frac{d^3 p_l}{2E_l} \quad (3.14)$$

with  $n_j$  the number of particles in the state  $|n\rangle$  (we can also consider a sum over final spin states, colours etc.). Let's suppose that the initial and final states are the same:

$$\langle i|\mathcal{M}^\dagger|n\rangle \langle n|\mathcal{M}|i\rangle = \langle n|\mathcal{M}|i\rangle^\dagger \langle n|\mathcal{M}|i\rangle = \left( (2\pi)\delta^{(4)}(\mathcal{P}_i - \mathcal{P}_n) \right)^2 |\mathcal{M}_{i \rightarrow n}|^2 \quad (3.15)$$

Thus, we obtain the standard form of the Optical Theorem:

$$-2Im(\mathcal{M}_{i \rightarrow i}) = \sum_n \frac{1}{(2\pi)^{3n_j-4}} \int \prod_{l=1}^{n_j} \frac{d^3 p_l}{2E_l} \delta^{(4)}(\mathcal{P}_i - \mathcal{P}_n) |\mathcal{M}_{i \rightarrow n}|^2 \quad (3.16)$$

If the initial state is a two particle state, then we are dealing with elastic scattering and the theorem takes the form:

$$-2Im(\overline{\sum} \mathcal{M}_{i \rightarrow i}) = 2\lambda^{1/2}(s, m_a^2, m_b^2) \sum_n \sigma(a + b \rightarrow n) = 2\lambda^{1/2} \sigma(a + b \rightarrow all) \quad (3.17)$$

If the initial state is a one particle state, we are dealing with self energy diagrams therefore:

$$-2Im(\overline{\sum} \mathcal{M}_{i \rightarrow i}) = 2M_a \sum_n \Gamma(a \rightarrow n) = 2M_a \Gamma(a \rightarrow all) \quad (3.18)$$

If we apply this to one of our Higgs self energy diagrams, (with no tadpoles) the theorem tells us:

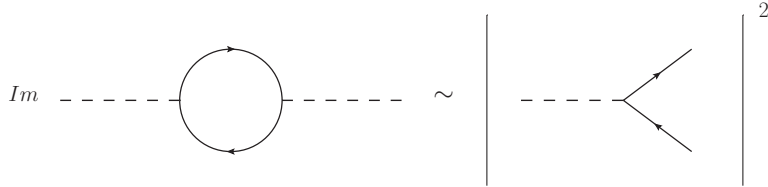


Figure 43: Diagrammatic representation for the Optical Theorem.

This justifies the modification that we made in the W and Z propagators (1.86) when we were analyzing the Higgs main decay channels. The next section will be dedicated to the calculation of the Higgs self-energy diagrams one by one.

### 3.2 Self Energy diagrams

Now we can proceed to calculate the Higgs self-energy diagrams, one by one, in order to obtain the needed quantum correction for the cross section.

Higgs self-energy first diagram:

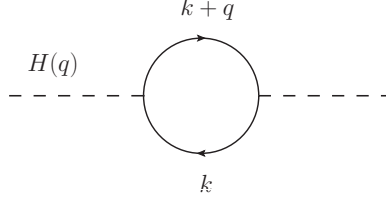


Figure 44: Higgs self-energy contribution coming from the top quark.

$$i\Pi^{(t)}(q^2) \equiv -N_C \frac{m^2}{v^2} \int \frac{d^D k}{(2\pi)^D} \frac{\text{Tr}\{(\not{k} + \not{q} + m)(\not{k} + m)\}}{(k^2 - m^2)[(k+q)^2 - m^2]} \quad (3.19)$$

Spinor trace in D dimensions:

$$\text{Tr}\{(\not{p} + \not{q} + m)(\not{k} + m)\} = 4(k^2 + m^2 + kq) \quad (3.20)$$

Feynman parametrization of the propagator:

$$\frac{1}{AB} = \int_0^1 dx \frac{1}{[Ax + B(1-x)]^2} \quad (3.21)$$

Taking  $A = (k+q)^2 - m^2$  and  $B = k^2 - m^2$  we get:

$$\frac{1}{(k^2 - m^2)[(k+q)^2 - m^2]} = \int_0^1 dx \frac{1}{[(k+qx)^2 - a^2]^2} \quad (3.22)$$

where we have defined  $\mathbf{a}^2 \equiv -\mathbf{q}^2 \mathbf{x}(1-\mathbf{x}) + \mathbf{m}^2 - i\epsilon$ . We obtain the following expression:

$$i\Pi^{(t)}(q^2) = -N_C \frac{4m^2}{v^2} \int_0^1 dx \int \frac{d^D k}{(2\pi)^D} \frac{k^2 + m^2 + kq}{[(k+qx)^2 - a^2]^2} \quad (3.23)$$

After performing the variable shift  $k \rightarrow k + xq$  and eliminating all the linear terms in  $k^\mu$  we obtain:

$$i\Pi^{(t)}(q^2) = -N_C \frac{4m^2}{v^2} \int_0^1 dx \int \frac{d^D k}{(2\pi)^D} \frac{k^2 + a^2}{[k^2 - a^2]^2} \quad (3.24)$$

Let us compute the first term:

$$\int_0^1 dx \int \frac{d^D k}{(2\pi)^D} \frac{k^2}{[k^2 - a^2]^2} = \int_0^1 dx J(D, 1, 2, a^2) = \int_0^1 dx \frac{a^2 D}{D-2} J(D, 0, 2, a^2) \quad (3.25)$$

The second term that we have is:

$$\int_0^1 dx \int \frac{d^D k}{(2\pi)^D} \frac{a^2}{[k^2 - a^2]^2} = \int_0^1 dx a^2 J(D, 0, 2, a^2) \quad (3.26)$$

We take D to be  $\mathbf{D} = \mathbf{4} + \mathbf{2}\epsilon$ , therefore our expression of  $\Pi^{(t)}(q^2)$  becomes:

$$i\Pi^{(t)}(q^2) = -N_C \frac{4m^2}{v^2} \int_0^1 dx (3 - \epsilon) a^2 J(D, 0, 2, a^2) + O(\epsilon^2) \quad (3.27)$$

It is immediate to show that  $J(D, 0, 2, a^2)$  is equal to:

$$J(D, 0, 2, a^2) = \frac{-i}{(4\pi)^2} \mu^{2\epsilon} \left( \frac{1}{\hat{\epsilon}} + \ln \left( \frac{a^2}{\mu^2} \right) + O(\epsilon) \right) \quad (3.28)$$

where we have defined  $1/\hat{\epsilon} \equiv 1/\epsilon + \gamma_E - \ln(4\pi)$ , with  $\gamma_E$  the Euler-Mascheroni constant and  $1/\epsilon$  the Euler gamma function pole. Up to  $O(\epsilon)$  we have:

$$\Pi^{(t)}(q^2) = N_C \frac{12m^2}{(4\pi v)^2} \mu^{2\epsilon} \int_0^1 dx a^2 \left( \frac{1}{\hat{\epsilon}} + \ln \left( \frac{a^2}{\mu^2} \right) - \frac{1}{3} \right) \quad (3.29)$$

Let's calculate the integral:

$$\int_0^1 dx a^2 = \int_0^1 dx (-q^2 x(1-x) + m^2) = m^2 - \frac{q^2}{6} \quad (3.30)$$

Thus, we can write the following:

$$\Pi^{(t)}(q^2) = N_C \frac{12m^2}{(4\pi v)^2} \mu^{2\epsilon} \left[ \frac{1}{\hat{\epsilon}} \left( m^2 - \frac{q^2}{6} \right) + \frac{q^2}{18} - \frac{m^2}{3} + \int_0^1 dx a^2 \ln \left( \frac{a^2}{\mu^2} \right) \right] \quad (3.31)$$

Using the  $\overline{MS}$  scheme we obtain:

$$\begin{aligned} \Pi_\epsilon^{(t)}(\mu) &= N_C \frac{12m^2}{(4\pi v)^2} \mu^{2\epsilon} \left( m^2 - \frac{q^2}{6} \right) \frac{1}{\hat{\epsilon}} \\ \Pi_R^{(t)}(q, \mu) &= N_C \frac{12m^2}{(4\pi v)^2} \left( \frac{q^2}{18} - \frac{m^2}{3} + \int_0^1 dx a^2 \ln \left( \frac{a^2}{\mu^2} \right) \right) \end{aligned} \quad (3.32)$$

After calculating the first Higgs energy diagram we can use its explicit expression to check on the optical theorem we have deduced previously. The only piece of  $\Pi_R^{(t)}$  that develops an imaginary part is the one defined below:

$$\begin{aligned} T(q^2, m^2) &= N_C \frac{12m^2}{(4\pi v)^2} \int_0^1 dx a^2 \ln \left( \frac{a^2}{\mu^2} \right) \\ &= N_C \frac{12m^2}{(4\pi v)^2} \int_0^1 dx [-q^2 x(1-x) + m^2] \ln \left( \frac{-q^2 x(1-x) + m^2 - i\epsilon}{\mu^2} \right) \end{aligned} \quad (3.33)$$

In order to find the imaginary part we have to find the roots of the equation:

$$-q^2 x(1-x) + m^2 = 0 \Rightarrow x_{1,2} = \frac{1}{2} \pm \frac{1}{2} \sqrt{1 - \frac{4m^2}{q^2}} \quad (3.34)$$

In the region in between  $x_1$  and  $x_2$  the logarithm's only imaginary part is the one that comes from  $-i\epsilon$ , and it is  $\pm i\pi$  depending on the sign rules we adopt. So, except a global sign we find:

$$-\pi N_C \frac{12m^2}{(4\pi v)^2} \int_{x_2}^{x_1} dx [-q^2 x(1-x) + m^2] = \frac{N_C m^2}{8\pi v^2} q^2 \left( 1 - \frac{4m^2}{q^2} \right)^{3/2} \quad (3.35)$$

We finally obtain that:

$$Im(\Pi^{(t)}(q^2 = M_H^2)) = M_H \Gamma(H \rightarrow t\bar{t}) \quad (3.36)$$

and this is exactly what we were intending to prove. We should also observe here that, as expected, the imaginary part does not depend on the renormalization scale  $\mu$ .

Now let us take a look at another Higgs self energy process:

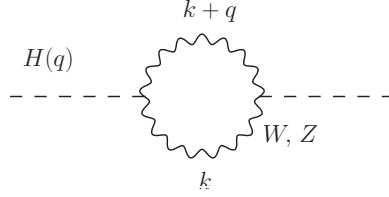


Figure 45: Higgs self-energy contribution coming from weak vector bosons.

We shall calculate the process for a W boson. The same result is valid for a Z boson by only changing the masses and multiplying by a 1/2 symmetry factor; ( $k' \equiv k + q$ ):

$$\begin{aligned}
i\Pi^{(W_1)}(q^2) &= \frac{4M_W^4}{v^2} \int \frac{d^D k}{(2\pi)^D} \left( -g_{\mu\nu} + \frac{k_\mu k_\nu}{M_W^2} \right) \left( -g^{\mu\nu} + \frac{k'^\mu k'^\nu}{M_W^2} \right) \frac{1}{(k^2 - M_W^2)[(k+q)^2 - M_W^2]} \\
&= \frac{4}{v^2} \int \frac{d^D k}{(2\pi)^D} \frac{(k^2 + kq)^2 - M_W^2(2k^2 + q^2 + 2kq) + D M_W^4}{(k^2 - M_W^2)[(k+q)^2 - M_W^2]} \quad (3.37)
\end{aligned}$$

We have the same propagators as in the previous case so, using the same Feynman parameterization this time using the letter  $\mathbf{b}^2 \equiv -\mathbf{q}^2 \mathbf{x}(\mathbf{1} - \mathbf{x}) + M_W^2$  we get:

$$\begin{aligned}
i\Pi^{(W_1)}(q^2) &= \frac{4}{v^2} \int_0^1 dx \int \frac{d^D k}{(2\pi)^D} \frac{(k^2)^2 + (kq)^2 + 2k^2(kq) - M_W^2(2k^2 + q^2 + 2kq) + D M_W^4}{[(k+qx)^2 - b^2]^2} \\
&= \frac{4}{v^2} \int_0^1 dx \int \frac{d^D k}{(2\pi)^D} \frac{1}{[k^2 - b^2]^2} \left\{ (k^2)^2 + (q^2)^2 x^2 (x-1)^2 + 2k^2 q^2 x(x-1) + \right. \\
&\quad \left. (1-2x)^2 (kq)^2 - 2M_W^2 k^2 - M_W^2 q^2 (2x^2 - 2x + 1) + D M_W^4 \right\} \quad (3.38)
\end{aligned}$$

As we have seen in the previous sections we can make the following substitutions:

$$(kq)^2 = k^\mu k^\nu q_\mu q_\nu \rightarrow \frac{g^{\mu\nu}}{D} k^2 q_\mu q_\nu = \frac{q^2}{D} k^2 \quad (3.39)$$

Rearranging terms we get to the following:

$$\begin{aligned}
i\Pi^{(W_1)}(q^2) &= \frac{4}{v^2} \int_0^1 dx \int \frac{d^D k}{(2\pi)^D} \frac{1}{[k^2 - b^2]^2} \left\{ k^2 \left( 2q^2 x(x-1) + \frac{q^2}{D} (1-2x)^2 - 2M_W^2 \right) \right. \\
&\quad \left. + (k^2)^2 + (q^2)^2 x^2 (x-1)^2 - M_W^2 q^2 (2x^2 - 2x + 1) + D M_W^4 \right\} \\
&= \frac{4}{v^2} \int_0^1 dx \left\{ J(D, 1, 2, b^2) \left( 2q^2 x(x-1) + \frac{q^2}{D} (1-2x)^2 - 2M_W^2 \right) + J(D, 2, 2, b^2) \right. \\
&\quad \left. + J(D, 0, 2, b^2) \left( (q^2)^2 x^2 (x-1)^2 - M_W^2 q^2 (2x^2 - 2x + 1) + D M_W^4 \right) \right\} \quad (3.40)
\end{aligned}$$

Using Euler's gamma function properties it is easy to find:

$$\begin{aligned}
J(D, 1, 2, b^2) &= \frac{b^2 D}{D-2} J(D, 0, 2, b^2) \\
J(D, 2, 2, b^2) &= \frac{b^2(D+2)}{D} J(D, 1, 2, b^2) = \frac{b^4(D+2)}{D-2} J(D, 0, 2, b^2) \quad (3.41)
\end{aligned}$$

Grouping terms, we can express  $i\Pi^{(W_1)}(q^2)$  as:

$$\begin{aligned}
i\Pi^{(W_1)}(q^2) &= \frac{4}{v^2} \int_0^1 dx \left\{ J(D, 0, 2, b^2) \frac{b^2 D}{D-2} \left( 2q^2 x(x-1) + \frac{q^2}{D} (1-2x)^2 - 2M_W^2 \right) \right. \\
&\quad + J(D, 0, 2, b^2) \left( (q^2)^2 x^2 (x-1)^2 - M_W^2 q^2 (2x^2 - 2x + 1) + D M_W^4 \right) \\
&\quad \left. + J(D, 0, 2, b^2) \frac{b^4 (D+2)}{D-2} \right\} \\
&= \frac{4}{v^2} \int_0^1 dx J(D, 0, 2, b^2) \left\{ \frac{b^2 D}{D-2} \left( 2q^2 x(x-1) + \frac{q^2}{D} (1-2x)^2 - 2M_W^2 \right) \right. \\
&\quad \left. + (q^2)^2 x^2 (x-1)^2 - M_W^2 q^2 (2x^2 - 2x + 1) + D M_W^4 + \frac{b^4 (D+2)}{D-2} \right\} \tag{3.42}
\end{aligned}$$

Taking as usual  $D = 4 + 2\epsilon$ , then up to order  $\epsilon$  we have:

$$\begin{aligned}
i\Pi^{(W_1)}(q^2) &= \frac{4}{v^2} \int_0^1 dx J(D, 0, 2, b^2) \left\{ b^2 (2 - \epsilon) \left( 2q^2 x(x-1) + \frac{2-\epsilon}{8} q^2 (1-2x)^2 - 2M_W^2 \right) \right. \\
&\quad \left. + (q^2)^2 x^2 (x-1)^2 - M_W^2 q^2 (2x^2 - 2x + 1) + (4 + 2\epsilon) M_W^4 + b^4 (3 - 2\epsilon) \right\} \tag{3.43}
\end{aligned}$$

We have seen that we can express  $J(D, 0, 2, b^2)$  in terms of the Gamma function pole as:

$$J(D, 0, 2, b^2) = \frac{-i}{(4\pi)^2} \mu^{2\epsilon} \left( \frac{1}{\hat{\epsilon}} + \ln \left( \frac{a^2}{\mu^2} \right) + O(\epsilon) \right) \tag{3.44}$$

We obtain:

$$\begin{aligned}
i\Pi^{(W_1)}(q^2) &= \frac{-4i}{(4\pi v)^2} \mu^{2\epsilon} \int_0^1 dx \left( \frac{1}{\hat{\epsilon}} + \ln \left( \frac{b^2}{\mu^2} \right) \right) \left\{ b^2 (2 - \epsilon) \left( 2q^2 x(x-1) - 2M_W^2 \right) \right. \\
&\quad + \frac{b^2}{2} (1 - \epsilon) q^2 (1 - 2x)^2 + (q^2)^2 x^2 (x-1)^2 - M_W^2 q^2 (2x^2 - 2x + 1) \\
&\quad \left. + (4 + 2\epsilon) M_W^4 + b^4 (3 - 2\epsilon) \right\} \tag{3.45}
\end{aligned}$$

In order to simplify our calculation we need to make some definitions:

$$\begin{aligned}
A &\equiv b^2 (2q^2 x(x-1) - 2M_W^2) \\
B &\equiv \frac{b^2}{2} q^2 (1-2x)^2 \\
C &\equiv (q^2)^2 x^2 (x-1)^2 - M_W^2 q^2 (2x^2 - 2x + 1) \\
E &\equiv M_W^4 \\
F &\equiv b^4 \tag{3.46}
\end{aligned}$$

We find the following expression.

$$\begin{aligned}
i\Pi^{(W_1)}(q^2) &= \frac{-4i}{(4\pi v)^2} \mu^{2\epsilon} \int_0^1 dx \frac{1}{\hat{\epsilon}} (2A + B + C + 4E + 3F) \\
&\quad + \frac{-4i}{(4\pi v)^2} \mu^{2\epsilon} \int_0^1 dx (-A - B + 2E - 2F) \\
&\quad + \frac{-4i}{(4\pi v)^2} \mu^{2\epsilon} \int_0^1 dx \ln \left( \frac{b^2}{\mu^2} \right) (2A + B + C + 4E + 3F) \tag{3.47}
\end{aligned}$$

Performing some integrals:

$$\begin{aligned}
\int_0^1 dx A &= \frac{(q^2)^2}{15} - 2M_W^4 \\
\int_0^1 dx B &= \frac{1}{6}M_W^2 q^2 - \frac{(q^2)^2}{60} \\
\int_0^1 dx C &= -\frac{2}{3}M_W^2 q^2 + \frac{(q^2)^2}{30} \\
\int_0^1 dx E &= E = M_W^4 \\
\int_0^1 dx F &= M_W^4 - \frac{q^2 M_W^2}{3} + \frac{(q^2)^2}{30}
\end{aligned} \tag{3.48}$$

Therefore we find the following expressions:

$$\begin{aligned}
\Pi_\epsilon^{(W_1)}(q^2) &= \frac{-\mu^{2\epsilon}}{(4\pi v)^2} \frac{1}{\hat{\epsilon}} \left( 12M_W^4 - 6q^2 M_W^2 + (q^2)^2 \right) \\
\Pi_R^{(W_1)}(q^2) &= \frac{-4}{(4\pi v)^2} \left( 2M_W^4 + \frac{1}{2}q^2 M_W^2 - \frac{7}{60}(q^2)^2 \right) \\
&\quad + \frac{-4}{(4\pi v)^2} \int_0^1 dx \ln\left(\frac{b^2}{\mu^2}\right) (2A + B + C + 4E + 3F)
\end{aligned} \tag{3.49}$$

So, for the Z diagram we obtain:

$$\begin{aligned}
\Pi_\epsilon^{(Z_1)}(q^2) &= \left(\frac{1}{2}\right) \frac{-\mu^{2\epsilon}}{(4\pi v)^2} \frac{1}{\hat{\epsilon}} \left( 12M_Z^4 - 6q^2 M_Z^2 + (q^2)^2 \right) \\
\Pi_R^{(Z_1)}(q^2) &= \left(\frac{1}{2}\right) \frac{-4}{(4\pi v)^2} \left( 2M_Z^4 + \frac{1}{2}q^2 M_Z^2 - \frac{7}{60}(q^2)^2 \right) \\
&\quad + \left(\frac{1}{2}\right) \frac{-4}{(4\pi v)^2} \int_0^1 dx \ln\left(\frac{b'^2}{\mu^2}\right) (2A + B + C + 4E + 3F)
\end{aligned} \tag{3.50}$$

where  $\mathbf{b}'^2 \equiv -\mathbf{q}^2 \mathbf{x}(1 - \mathbf{x}) + \mathbf{M}_Z^2$ .

Now, to find the imaginary part, we have to integrate the piece that contains the logarithm over the limits  $x_{1,2} = 1/2 \pm (1/2)(1 - 4M_W^2/q^2)^{1/2}$ . We obtain the following result:

$$\begin{aligned}
-\pi \frac{-4}{(4\pi v)^2} \int_{x_2}^{x_1} dx (2A + B + C + 4E + 3F) &= \frac{1}{4\pi v^2} \frac{1}{4} \left( 1 - \frac{4M_W^2}{q^2} \right)^{1/2} (12M_W^4 - 4q^2 M_W^2 + q^4) \\
&= \frac{M_W^4}{4\pi v^2} \left( 1 - \frac{4M_W^2}{q^2} \right)^{1/2} \left( 3 - \frac{q^2}{M_W^2} + \frac{q^4}{4M_W^4} \right)
\end{aligned} \tag{3.51}$$

Again we obtain a direct confirmation of the optical theorem:

$$\text{Im}(\Pi^{(W_1)}(q^2 = M_H^2)) = M_H \Gamma(H \rightarrow WW) \tag{3.52}$$

The next process that we look at is the self-Higgs interaction:

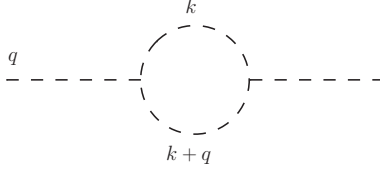


Figure 46: Higgs self-energy first contribution from self Higgs interaction.

$$\begin{aligned}
i\Pi^{(H_1)}(q^2) &= \frac{3!3!}{2!} \left(\frac{M^2}{2v}\right)^2 \int \frac{d^D k}{(2\pi)^D} \frac{1}{[k^2 - M^2][(k+q)^2 - M^2]} \\
&= \frac{9M^4}{2v^2} \int_0^1 dx \int \frac{d^D k}{(2\pi)^D} \frac{1}{[(k+xq)^2 - c^2]^2} \\
&= \frac{9M^4}{2v^2} \int_0^1 dx \int \frac{d^D k}{(2\pi)^D} \frac{1}{[k^2 - c^2]^2} \\
&= \frac{9M^4}{2v^2} \int_0^1 dx J(D, 0, 2, c^2) \\
&= \frac{9M^4}{2v^2} \int_0^1 dx \frac{-i}{(4\pi)^2} \mu^{2\epsilon} \left(\frac{1}{\hat{\epsilon}} + \ln\left(\frac{c^2}{\mu^2}\right) + O(\epsilon)\right) \\
&= \frac{-i}{(4\pi)^2} \mu^{2\epsilon} \frac{9M^4}{2v^2} \left(\frac{1}{\hat{\epsilon}} + \int_0^1 dx \ln\left(\frac{c^2}{\mu^2}\right)\right)
\end{aligned} \tag{3.53}$$

where we have defined  $\mathbf{c}^2 \equiv -\mathbf{q}^2 \mathbf{x}(1-\mathbf{x}) + \mathbf{M}^2$ . Using the  $\overline{MS}$  scheme we obtain:

$$\begin{aligned}
\Pi_\epsilon^{(H_1)}(\mu) &= -\frac{9M^4}{2} \frac{\mu^{2\epsilon}}{(4\pi v)^2} \frac{1}{\hat{\epsilon}} \\
\Pi_R^{(H_1)}(q, \mu) &= -\frac{9M^4}{2} \frac{1}{(4\pi v)^2} \int_0^1 dx \ln\left(\frac{c^2}{\mu^2}\right)
\end{aligned} \tag{3.54}$$

Calculating the last integral we find that the argument of the logarithm is always positive, therefore this diagram has no imaginary part. This is exactly what we were expecting for because  $\Gamma(H \rightarrow 2H)$  does not exist due to the kinematical restrictions  $q^2 < 4M^2$ .

We will deal now with the next set of diagrams (tadpoles). The first one is the second W diagram. The one corresponding to the Z boson will have the same expression, except for the usual 1/2 symmetry factor.

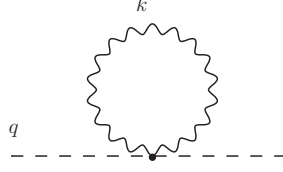


Figure 47: Higgs self-energy second contribution coming from weak bosons.

$$\begin{aligned}
i\Pi^{(W_2)} &= \frac{2M_W^2}{v^2} \int \frac{d^D k}{(2\pi)^D} \left( -g_\mu^\mu + \frac{k_\mu k^\mu}{M_W^2} \right) \frac{i^2}{k^2 - M_W^2} \\
&= -\frac{2}{v^2} \int \frac{d^D k}{(2\pi)^D} \frac{-DM_W^2 + k^2}{k^2 - M_W^2} \\
&= -\frac{2}{v^2} \{ -DM_W^2 J(D, 0, 1, M_W^2) + J(D, 1, 1, M_W^2) \}
\end{aligned} \tag{3.55}$$

It is easy to show that:

$$\frac{J(D, 1, 1, M_W^2)}{J(D, 0, 2, M_W^2)} = \frac{M_W^4}{D/2 - 1}; \quad \frac{J(D, 0, 1, M_W^2)}{J(D, 0, 2, M_W^2)} = \frac{M_W^2}{D/2 - 1} \tag{3.56}$$

Therefore, we have the following:

$$\begin{aligned}
i\Pi^{(W_2)} &= -\frac{2}{v^2} M_W^4 \left( \frac{1-D}{D/2-1} \right) J(D, 0, 2, M_W^2) \\
&= \frac{2}{v^2} M_W^4 (-\epsilon + 3) \frac{-i}{(4\pi)^2} \mu^{2\epsilon} \left( \frac{1}{\hat{\epsilon}} + \ln \left( \frac{M_W^2}{\mu^2} \right) + O(\epsilon) \right)
\end{aligned} \tag{3.57}$$

So we can write the following expression for this process:

$$\Pi^{(W_2)} = \frac{-\mu^{2\epsilon}}{(4\pi v)^2} M_W^4 (-2\epsilon + 6) \left( \frac{1}{\hat{\epsilon}} + \ln \left( \frac{M_W^2}{\mu^2} \right) + O(\epsilon) \right) \tag{3.58}$$

Thus, we find the following expression for the infinite and renormalized parts of the diagram:

$$\begin{aligned}
\Pi_\epsilon^{(W_2)} &= \frac{-\mu^{2\epsilon}}{(4\pi v)^2} \frac{1}{\hat{\epsilon}} 6M_W^4 \\
\Pi_R^{(W_2)} &= \frac{-4}{(4\pi v)^2} \left( \frac{3M_W^4}{2} \ln \left( \frac{M_W^2}{\mu^2} \right) - \frac{M_W^4}{2} \right)
\end{aligned} \tag{3.59}$$

As expected, the result does not depend on  $q^2$  and it does not have an imaginary part. For the Z diagram we have:

$$\begin{aligned}
\Pi_\epsilon^{(Z_2)} &= \frac{-\mu^{2\epsilon}}{(4\pi v)^2} \frac{1}{\hat{\epsilon}} 3M_Z^4 \\
\Pi_R^{(Z_2)} &= \frac{-4}{(4\pi v)^2} \left( \frac{3M_Z^4}{4} \ln \left( \frac{M_Z^2}{\mu^2} \right) - \frac{M_Z^4}{4} \right)
\end{aligned} \tag{3.60}$$

The next processes that we are going to look at are the Higgs self-energy tadpole diagrams due to self-Higgs interactions:

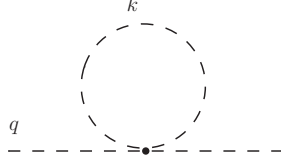


Figure 48: Higgs self-energy second contribution coming from self Higgs interactions.

$$i\Pi^{(H_2)} = \frac{3M^2}{2v^2} \int \frac{d^D k}{(2\pi)^D} \frac{-i^2}{k^2 - M^2} = \frac{3M^2}{2v^2} J(D, 0, 1, M^2) \quad (3.61)$$

We can easily find that:

$$J(D, 0, 1, M^2) = \frac{2M^2}{D-2} J(D, 0, 2, M^2) = M^2(1-\epsilon) \frac{-i}{(4\pi)^2} \mu^{2\epsilon} \left( \frac{1}{\hat{\epsilon}} + \ln\left(\frac{M^2}{\mu^2}\right) + O(\epsilon^2) \right) \quad (3.62)$$

Therefore, the expression for this diagram is simply:

$$i\Pi^{(H_2)} = \frac{-i}{(4\pi v)^2} \frac{3M^4}{2} \mu^{2\epsilon} \left( \frac{1}{\hat{\epsilon}} + \ln\left(\frac{M^2}{\mu^2}\right) - 1 \right) \quad (3.63)$$

The infinite and the renormalized part, then, read:

$$\begin{aligned} \Pi_\epsilon^{(H_2)} &= \frac{-1}{(4\pi v)^2} \frac{3M^4}{2} \mu^{2\epsilon} \frac{1}{\hat{\epsilon}} \\ \Pi_R^{(H_2)} &= \frac{-1}{(4\pi v)^2} \frac{3M^4}{2} \left( \ln\left(\frac{M^2}{\mu^2}\right) - 1 \right) \end{aligned} \quad (3.64)$$

The second tadpole diagram is:

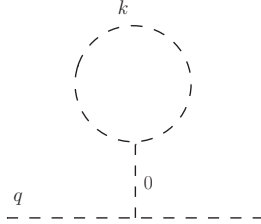


Figure 49: Higgs self-energy third contribution from Higgs self interactions.

$$i\Pi^{(H_3)} = \frac{3!3!}{2} \frac{M^4}{4v^2} \frac{1}{-M^2} \int \frac{d^D k}{(2\pi)^D} \frac{1}{k^2 - M^2} = -\frac{9M^2}{v^2} J(D, 0, 1, M^2) \quad (3.65)$$

The result is straightforward:

$$\begin{aligned} \Pi_\epsilon^{(H_3)} &= \frac{1}{(4\pi v)^2} \frac{9M^4}{2} \mu^{2\epsilon} \frac{1}{\hat{\epsilon}} \\ \Pi_R^{(H_3)} &= \frac{1}{(4\pi v)^2} \frac{9M^4}{2} \left( \ln\left(\frac{M^2}{\mu^2}\right) - 1 \right) \end{aligned} \quad (3.66)$$

The second W tadpole diagram that we have is:

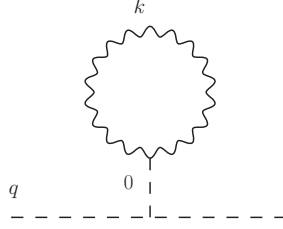


Figure 50: Higgs self-energy third contribution from weak bosons.

$$i\Pi^{(W_3)} = \frac{3!}{2} \frac{2M_W^2}{v^2} \int \frac{d^D k}{(2\pi)^D} \left( -g_\mu^\mu + \frac{k_\mu k^\mu}{M_W^2} \right) \frac{1}{k^2 - M_W^2} \quad (3.67)$$

Thus we have the following results for the W diagram:

$$\begin{aligned} \Pi_\epsilon^{(W_3)} &= \frac{\mu^{2\epsilon}}{(4\pi v)^2} \frac{1}{\hat{\epsilon}} 18M_W^4 \\ \Pi_R^{(W_3)} &= \frac{4}{(4\pi v)^2} \left( \frac{9M_W^4}{2} \ln \left( \frac{M_W^2}{\mu^2} \right) - \frac{3M_W^4}{2} \right) \end{aligned} \quad (3.68)$$

For the Z diagram we have:

$$\begin{aligned} \Pi_\epsilon^{(Z_3)} &= \frac{\mu^{2\epsilon}}{(4\pi v)^2} \frac{1}{\hat{\epsilon}} 9M_Z^4 \\ \Pi_R^{(Z_3)} &= \frac{4}{(4\pi v)^2} \left( \frac{9M_Z^4}{4} \ln \left( \frac{M_Z^2}{\mu^2} \right) - \frac{3M_Z^4}{4} \right) \end{aligned} \quad (3.69)$$

As for the top tadpole we have:

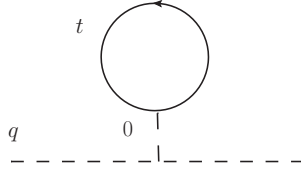


Figure 51: Higgs self-energy second contribution from the top quark.

$$i\Pi^{(t,2)} = \frac{3!}{2} N_C \frac{m}{v^2} \int \frac{d^D k}{(2\pi)^D} \frac{\text{Tr}\{\not{k} + m\}}{k^2 - m^2} = 12 N_C \frac{m^2}{v^2} \int \frac{d^D k}{(2\pi)^D} \frac{1}{k^2 - m^2} \quad (3.70)$$

It is also straightforward that:

$$\begin{aligned} \Pi_\epsilon^{(t_2)} &= \frac{-1}{(4\pi v)^2} 12N_C m^4 \mu^{2\epsilon} \frac{1}{\hat{\epsilon}} \\ \Pi_R^{(t_2)} &= \frac{1}{(4\pi v)^2} 12N_C m^4 \left( \ln \left( \frac{m^2}{\mu^2} \right) - 1 \right) \end{aligned} \quad (3.71)$$

Now, we have all the necessary ingredients to analyze the Higgs boson running mass.

### 3.3 Higgs Running Mass

Remember that from the Higgs renormalization process we got to the following expression:

$$\frac{1}{q^2 - M_0^2 + \Pi(q^2)} = \frac{Z_1}{q^2 - M^2 + \Pi_R(q^2, \mu^2)} \quad (3.72)$$

To obtain the expression for the Higgs running mass we must make the following parameterization:

$$\Pi(q^2) = (q^2 - M^2)\Pi_1 + \Pi_2 \quad (3.73)$$

Now we are able to calculate  $Z_1$ ,  $Z_2$  and  $\delta M^2$ :

$$\begin{aligned} Z_1 &= \frac{(q^2 - M^2)(1 + \Pi_{1,R}) + \Pi_{2,R}}{q^2 - M_0^2 + \Pi} = \frac{(q^2 - M^2)(1 + \Pi_{1,R}) + \Pi_{2,R}}{q^2 - M^2 + \delta M^2 + \Pi} \\ &= \frac{(q^2 - M^2)(1 + \Pi_{1,R}) + \Pi_{2,R}}{q^2 - M^2} \left(1 - \frac{\delta M^2 + \Pi}{q^2 - M^2}\right) \\ &= \left(1 + \Pi_{1,R} + \frac{\Pi_{2,R}}{q^2 - M^2}\right) \left(1 - \Pi_1 - \frac{\delta M^2 + \Pi_2}{q^2 - M^2}\right) \\ &= 1 - \Pi_{1,\epsilon} - \frac{\delta M^2 + \Pi_{2,\epsilon}}{q^2 - M^2} \end{aligned} \quad (3.74)$$

thus, we define the following:

$$\delta M^2 = -\Pi_{2,\epsilon} \Rightarrow Z_1 = 1 - \Pi_{1,\epsilon} \Rightarrow Z_2 = 1 - \Pi_{1,\epsilon} + \frac{\Pi_{2,\epsilon}}{M_0^2} \quad (3.75)$$

The renormalization group equation:

$$\mu \frac{dM^2}{d\mu} = -M^2 \gamma = -M^2 \left( \gamma_1 \frac{1}{\pi} + \gamma_2 \left( \frac{1}{\pi} \right)^2 + \dots \right) \quad (3.76)$$

So far, we have found the following divergent parts of the Higgs self energy diagrams:

$$\begin{aligned} \Pi_\epsilon^{(t)} &= \frac{1}{\hat{\epsilon}} \frac{\mu^{2\epsilon}}{(4\pi v)^2} N_C 12m^2 \left( m^2 - \frac{q^2}{6} \right) \\ \Pi_\epsilon^{(W_1)} &= \frac{1}{\hat{\epsilon}} \frac{-\mu^{2\epsilon}}{(4\pi v)^2} \left( 12M_W^4 - 6q^2 M_W^2 + (q^2)^2 \right) \\ \Pi_\epsilon^{(Z_1)} &= \frac{1}{\hat{\epsilon}} \frac{-\mu^{2\epsilon}}{(4\pi v)^2} \left( 6M_W^4 - 3q^2 M_W^2 + \frac{1}{2}(q^2)^2 \right) \\ \Pi_\epsilon^{(H_1)} &= \frac{1}{\hat{\epsilon}} \frac{-\mu^{2\epsilon}}{(4\pi v)^2} \frac{9M^4}{2}; \quad \Pi_\epsilon^{(t_2)} = \frac{-1}{(4\pi v)^2} 12N_C m^4 \mu^{2\epsilon} \frac{1}{\hat{\epsilon}} \\ \Pi_\epsilon^{(H_2)} &= \frac{1}{\hat{\epsilon}} \frac{-\mu^{2\epsilon}}{(4\pi v)^2} \frac{3M^4}{2}; \quad \Pi_\epsilon^{(H_3)} = \frac{1}{(4\pi v)^2} \frac{9M^4}{2} \mu^{2\epsilon} \frac{1}{\hat{\epsilon}} \\ \Pi_\epsilon^{(W_2)} &= \frac{1}{\hat{\epsilon}} \frac{-\mu^{2\epsilon}}{(4\pi v)^2} 6M_W^4; \quad \Pi_\epsilon^{(Z_3)} = \frac{\mu^{2\epsilon}}{(4\pi v)^2} \frac{1}{\hat{\epsilon}} 9M_Z^4 \\ \Pi_\epsilon^{(Z_2)} &= \frac{1}{\hat{\epsilon}} \frac{-\mu^{2\epsilon}}{(4\pi v)^2} 3M_W^4; \quad \Pi_\epsilon^{(W_3)} = \frac{\mu^{2\epsilon}}{(4\pi v)^2} \frac{1}{\hat{\epsilon}} 18M_W^4 \end{aligned}$$

Now, we need to factorize  $\Pi_\epsilon(q^2)$  as we mentioned before:

$$\begin{aligned} \left( m^2 - \frac{q^2}{6} \right) &= -\frac{1}{6}(q^2 - M^2) + m^2 - \frac{M^2}{6} \\ (12M_W^4 - 6q^2 M_W^2 + (q^2)^2) &= (M^2 - 6M_W^2 + q^2)(q^2 - M^2) + M^4 - 6M_W^2 M^2 + 12M_W^4 \end{aligned} \quad (3.77)$$

So we finally find that:

$$M^2 = M_0^2 + \delta M^2 = M_0^2 - \Pi_{2,\epsilon} = M_0^2 + \frac{\mu^{2\epsilon}}{(4\pi v)^2} M_0^2 \left[ 2 N_C m^2 - 6M_W^2 - 3M_Z^2 + 3M_0^2 \right] \frac{1}{\epsilon} \quad (3.78)$$

Therefore, the renormalization group equation becomes:

$$\mu \frac{dM^2}{d\mu} = \frac{2M^2}{(4\pi v)^2} \left[ 2 N_C m^2 - 6M_W^2 - 3M_Z^2 + 3M^2 \right] \quad (3.79)$$

The solution to this at  $O(1/v^2)$  is:

$$\begin{aligned} M^2(\mu^2) &= M^2(\mu_0^2) + \frac{M^2(\mu_0^2)}{(4\pi v)^2} \left[ 2 N_C m^2(\mu_0^2) - 6M_W^2(\mu_0^2) - 3M_Z^2(\mu_0^2) + 3M^2(\mu_0^2) \right] \ln \left( \frac{\mu^2}{\mu_0^2} \right) \\ &\equiv M^2(\mu_0^2) + C(M_i^2, \mu_0) \frac{M^2(\mu_0)}{(4\pi v)^2} \ln \left( \frac{\mu^2}{\mu_0^2} \right) \end{aligned} \quad (3.80)$$

The interesting thing that we observe here is the Higgs mass dependence with all the other massive particles. This gives rise to the hierarchy and the fine tuning problem. If we consider that there is new physics at higher energies, than we can see the SM as an effective theory. If there is new physics at higher energies than there must be other massive particles and the Higgs boson would also have Yukawa couplings to them, in consequence, there would appear new terms in the Higgs renormalization corresponding to the new particles. Therefore, the Higgs mass could run to that scale. We say could because, it doesn't necessarily have to. In eq. (3.80) we see that the correction term to the Higgs mass is proportional to  $M_H^2$  and the terms contained in  $C(M_i^2)$  are quadratic. Therefore, for a small Higgs mass the correction term doesn't have to be big. The problem would arise, if somehow, the term  $C(M_i^2)$  contained terms proportional to  $M_N^4$  where  $M_N$  is a new heavy particle at higher energy scales. If this happend, how could we still have a low mass Higgs boson in our theory as all the electroweak precisions constraints (Section 4) indicate? In order for this mass to be small, tremendous cancellations would have to occur at higher orders (fine tuning). Moreover, if we impose this cancellation to occur at some order in perturbation theory, then we would obtain some conditions on the masses of the particles involved; if we go to higher orders this condition will be spoiled by new terms and some new conditions would appear. This means that the physics at the energy scale we are at now, depends on some finely tuned parameters, that, if modified, would give rise to a whole different world then the one we know. This is a generic problem of theories containing fundamental scalars. Super-Symmetry (SUSY) provides an elegant solution through the cancellation of fermionic and bosonic contributions. Unfortunately, no traces of SUSY have been found yet. The present experimental constraints imply that SUSY should be badly broken and the cancellations are no longer enforced by symmetry. Therefore, the fine tuning problem remains open.

## 4. Final Conclusions

As a final conclusion, let us talk a little bit about the electroweak precision fits and experimental mass exclusions for the Higgs boson. Precision electroweak measurements provide sensitivity to mass scales higher than the available experimental energies. This is done by exploiting contributions from quantum loops, for example, loops that involve a Higgs particle:

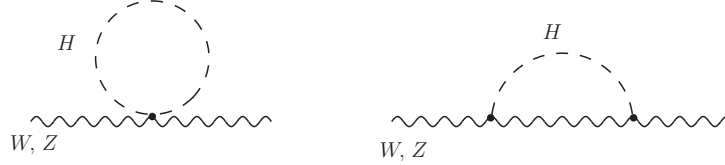


Figure 52: Some loops needed for electroweak precision fits.

This type of loop quantum corrections, with a proper choice of input parameters, allow us to give some constraints on the Higgs mass and other parameters. The basic inputs usually are  $\alpha(M_Z)$ ,  $G_F$  and  $M_Z$ . It is also a powerful tool to look for new physics; electroweak quantum corrections predicted correctly the mass of the top quark before its actual discovery. Let's discuss the following example equation [23]:

$$M_W^2 \left(1 - \frac{M_W^2}{M_Z^2}\right) = \frac{\pi\alpha}{\sqrt{2}G_F}(1 + \Delta r) \quad (3.81)$$

$\Delta r$  is a term that stands for the electroweak corrections. It contains a term proportional to  $\Delta\alpha$ , a negative term proportional to  $\mathbf{m}_t^2$  and another term proportional to  $\ln(\mathbf{M}_H)$ . Therefore, the electroweak precision fits are sensitive to the top mass and the Higgs mass. However, owing to an accidental  $SU(2)_C$  symmetry of the scalar sector (the so-called custodial symmetry), the constraints on the Higgs mass are much weaker than the ones on the top quark (logarithmic instead of quadratic). After its experimental measurement,  $m_t$  was used to put further constraints on the Higgs mass. The latest one [14], uses the  $\Delta\chi^2$  estimator to find the following: for a standard fit  $M_H = 96_{-24}^{+31}$  GeV and for a complete fit  $M_H = 120_{-15}^{+12}$  GeV, with the upper bounds 200 GeV (99 % CL standard fit) and 149 GeV (99 % CL complete fit) (Fig. 53). These results are quite sensitive to the input value of  $\alpha(M_Z^2)^{-1}$ ; using,  $\alpha(M_Z^2)^{-1} = 128.944 \pm 0.019$ , the result  $M_H = 88_{-23}^{+29}$  has been recently quoted [11]. With these data fits a fourth family of leptons and quarks is allowed with large  $M_H$  [14]. This is, of course, compatible with our conclusion from section 2.5. Five or more generation are disfavoured [14].

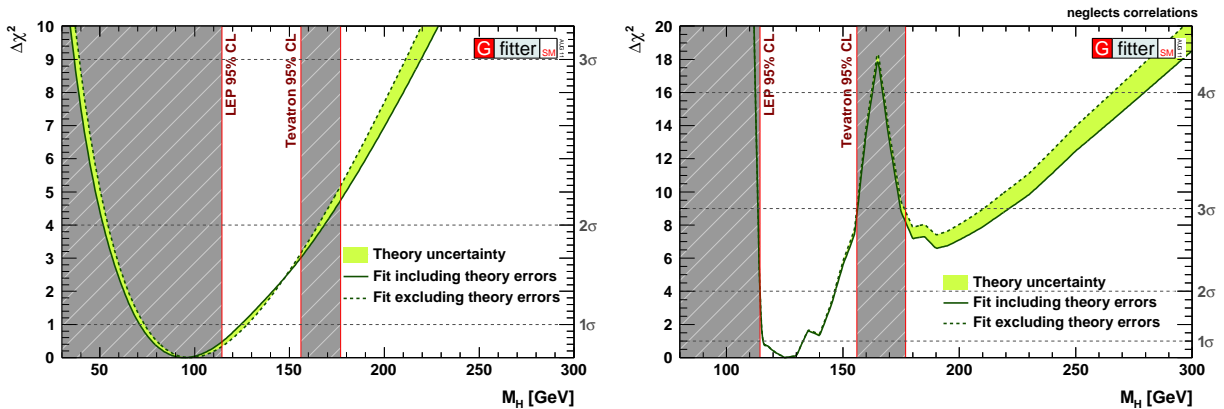


Figure 53:  $\Delta\chi^2$  as a function of  $M_H$  for the standard fit (left) and for the complete fit (right).

Now, let's take a look at the latest experimental mass exclusions at the LHC and Tevatron and LEP. The plot we see below shows the latest for Tevatron experimental limits on the Higgs production cross section, normalized to the Standard Model one, combining the CDF and D0 data [9] (Fig. 54). The Tevatron excluded regions at 95 % CL are  $156 < M_H < 177$  GeV and  $100 < M_H < 108$  GeV with luminosity in between 4.0 and 8.6  $\text{fb}^{-1}$ . The expected exclusion region with the current sensitivity is  $148 < M_H < 180$  GeV and  $100 < M_H < 109$  GeV. Very low Higgs masses, below 100 GeV were not studied. One of the most relevant conclusion that we can read in the same reference is that the sensitivity of this combined search is sufficient to exclude a high mass Higgs boson. This in agreement with the ATLAS collaboration, that, sees very stringent constraints for a Higgs mass above 250 GeV [7]. The LEP constraints on Higgs mass is  $M_H > 114.4$  GeV.

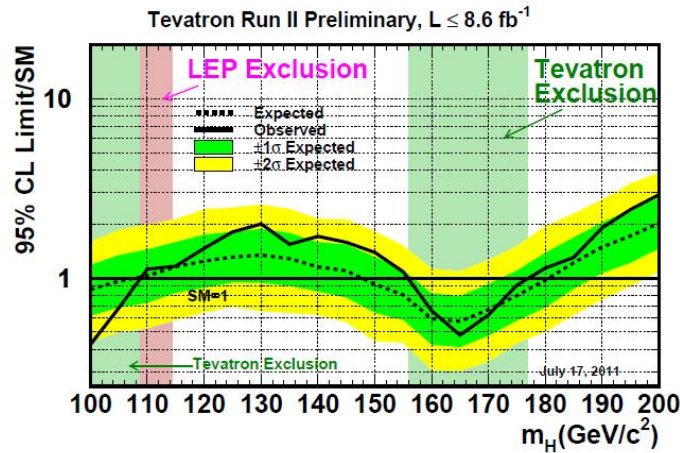


Figure 54: Higgs mass exclusions at Tevatron and LEP at 95% CL.

Let's now take a look at the exclusions provided by the combined ATLAS exclusion data at 1-1.7  $\text{fb}^{-1}$  [20]. The excluded regions are  $146 < M_H < 232$ ,  $256 < M_H < 282$  and  $296 < M_H < 466$ . We can also read [7] that they also exclude a fourth generation SM between 140 and 185 GeV. This exclusion is less stringent than the one from CMS.

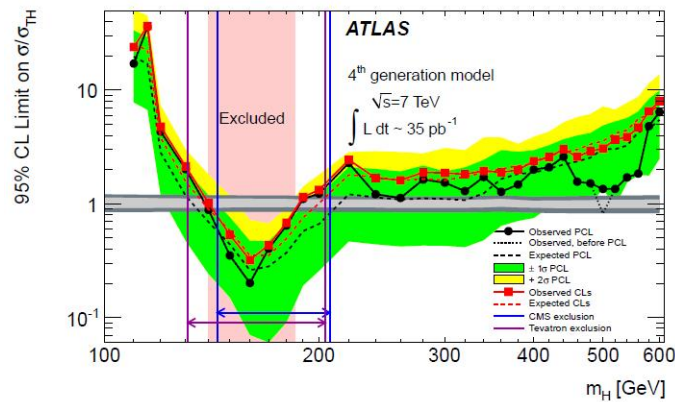


Figure 55: SM4 Higgs mass exclusions at ATLAS.

The CMS collaboration also provides three mass range exclusions [21] very similar to the ones from ATLAS (Fig.56). Their excluded mass ranges are  $145 < M_H < 216$ ,  $226 < M_H < 288$  and  $310 < M_H < 340$ .

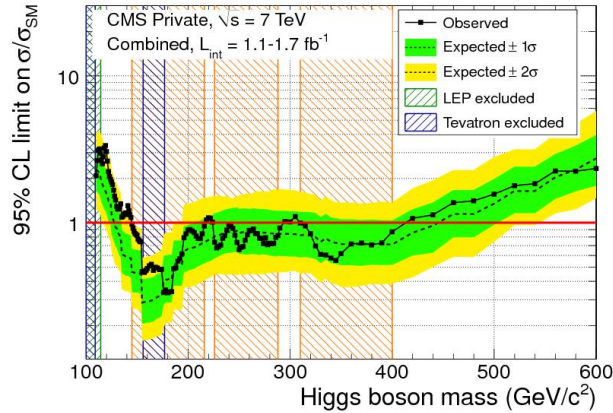


Figure 56: Higgs mass exclusions at CMS at 95% CL.

As we saw earlier, EW precision tests prefer a low mass SM Higgs. In Fig. 57 we show the remaining, non-excluded region for a low mass Higgs (white fringe). This remaining region is centered on the two photon region. We insisted in including this channel in our plot because its signal is the cleanest one. In this region the dominant decay is  $H \rightarrow b\bar{b}$  but with a large QCD background. All the other channels suffer from the same inconvenience except for the two photon decay. Moreover, the radiative corrections to the  $H \rightarrow \gamma\gamma$  decay width only affect the top quark loop. The W loop nor the final states are affected by higher order corrections [22]. These corrections are below 3% therefore, they are practically insignificant. These are the main reasons why this is the most promising decay channel in this region.

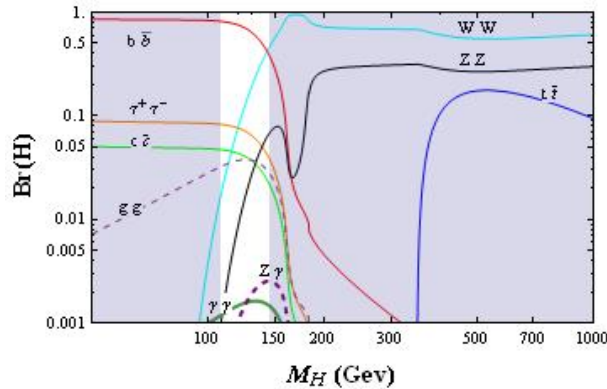


Figure 57: Non-excluded low mass Higgs region.

Perhaps, in one year or so we can definitely exclude a SM Higgs boson and discover new physics or, on the contrary, discover the SM Higgs boson and confirm the model. In any of these cases we need to go beyond the SM. Even with the discovery of the Higgs boson there are still going to be many unanswered questions. Why three generations? Why this type symmetry breaking? Why three colours of quarks? Why no quantum gravity? And what about neutrinos? There will still be many interesting new physics to discover. Even if the SM proves to be right, we must necessarily ask why the SM and not other symmetries? There will always be a bigger picture to be looking for.

## 5. References

- [1]. The Standard Model of Electroweak Interactions, A. Pich, arXiv:0705.4264v1 [hep-ph] 29 May 2007
- [2]. Foundations of Quantum Chromodynamics, T. Muta, World Scientific Lecture Notes in Physics - Vol. 78
- [3]. The Standard Model in the Making, D. Bardin and C. Passarino, Oxford Science Publications
- [4]. Weak Interactions and Modern Particle Theory, H. Georgi, Dover
- [5]. ECFA Large Hadron Collider Workshop. Proceeding Vol II, Editors: G. Jarlskog, D. Rein
- [6]. Gauge Theory of Elementary Particle Physics, Cheng and Lee, Oxford Scientific Publications
- [7]. Limits on the production of the Standard Model Higgs Boson in pp collisions at  $\sqrt{s} = 7$  TeV with the ATLAS detector, Atlas Collaboration, arXiv:1106.2748v2 [hep-ex] 4 June 2011
- [8]. Standard Model Higgs Boson Search Combination at CDF, Adrian Buzatu, McGill University, On behalf of the Collider Detector at Fermilab, EPS-HEP 2011, 22 July 2011
- [9]. Combined CDF and D0 Upper Limits on Standard Model Higgs Boson Production with up to  $8.6 fb^{-1}$  of Data, The TEVNPH Working Group for the CDF and D0 Collaborations, arXiv:1107.5518v1 [hep-ex] July 28 2011
- [10]. Combined ATLAS Standard Model Higgs Search with  $1 fb^{-1}$  of Data at 7 TeV, Kyle Cranmer, New York University on behalf of the ATLAS Collaboration, EPS-HEP 2011, July 2011
- [11].  $(g - 2)_\mu$  and  $\alpha(M_Z^2)$  re-evaluated using new precise data, Kaoru Hagiwarana, Ruofan Liaob, Alan D. Martinc, Daisuke Nomurad and Thomas Teubnerb, arXiv:1105.3149v2 [hep-ph] 5 Aug 2011
- [12]. Ruling out a fourth generation using limits on hadron collider Higgs signals, John F. Gunion, arXiv:1105.3965v2 [hep-ph] 23 May 2011
- [13]. Impact on the Higgs Production Cross Section and Decay Branching Fractions of Heavy Quarks and Leptons in a Fourth Generation Model, arXiv:1105.1634v2 [hep-ph] 11 May 2011
- [14]. The global electroweak fit and constraints on new physics, Matthias Schott (CERN) on behalf of the Gfitter Group, M. Baak, M. Goebel, J. Haller, A. Hocker, D. Ludwig, K. Mönig, M.S., J. Stelzer, EPS-HEP 2011, July 2011
- [15]. Combined results on SM Higgs Search with the CMS Detector CMS Collaboration, Andrey Korytov, EPS 2011 Grenoble
- [16]. The Anatomy of Electro-Weak Symmetry Breaking, Tome I: The Higgs boson in the Standard Model, Abdelhak DJOUADI, arXiv:hep-ph/0503172v2 3 May 2005
- [17]. Parton distributions for the LHC, A.D. Martina, W.J. Stirlingb, R.S. Thornec and G. Wattc, arXiv:0901.0002v3 [hep-ph] 7 Jul 2009
- [18]. Handbook of LHC Higgs cross sections, I. Inclusive observables, arXiv:1101.0593v3 [hep-ph] 20 May 2011
- [19]. Matthew Herndon, Annu. Rev. Nucl. Part. Sci. 2011.61. Downloaded from www.annualreviews.org

[20]. Higgs searches in ATLAS, Aleandro Nisati, INFN-Roma, Lepton-Photon Conference, Mumbai, August 2011

[21]. Search for the Higgs Boson with the CMS Detector, Vivek Sharama, University of California, San Diego, XXV International Symposium on Lepton & Photon Interactions at High Energies, Mumbai, August 2011

[22] Bernd A. Kniehl. Higgs phenomenology at one loop in the standard model. *Phys. Rept.*, 240:211-300, 1994

[23] Electroweak fits at LEP, E. Lancon. DAPNIA/SPP, CEASaclay, 91191 GifsurYvette Cedex, France

[24] [http://gfitter.desy.de/Standard\\_Model/](http://gfitter.desy.de/Standard_Model/)